Australian Government
Department of Defence
Defence Science and
Technology Organisation

Overview of STAP Algorithms

Yunhan Dong

Electronic Warfare and Radar Division
Defence Science and Technology Organisation

DSTO-TN-0992

ABSTRACT

This technical note reviews space-time adaptive processing (STAP) algorithms including various dimension-reduced, rank-reduced partial or sub-optimal variants as well as pseudo-STAP algorithms. Briefly examined are also knowledge-aided (KA) STAP and elevation-azimuth-time 3D STAP that further improve STAP performance, especially under the heterogeneous clutter environment and range ambiguous conditions. Imperfections of radar-platform system deteriorating performance and limiting detection algorithms are discussed. Requirements on data resource and computation by each algorithm are assessed and compared.

Published by

Electronic Warfare and Radar Division
DSTO Defence Science and Technology Organisation
PO Box 1500
Edinburgh South Australia 5111 Australia

Telephone: (08) 7389 5555
Fax: (08) 7389 6567

AR-014-950
March 2011

Overview of STAP Algorithms

Executive Summary

In support of the Australian Defence Force's acquisition of the Airborne Early Warning and Control (AEW&C) project and to improve the surveillance capability for its radar in the near future, this technical note reviews space-time adaptive processing (STAP) algorithms including various dimension-reduced, rank-reduced, partial-adaptive or sub-optimal variants, pseudo-STAP, knowledge-aided (KA) STAP, elevation-azimuth-time 3D STAP and so on. Imperfections of radar-platform system deteriorating performance and limiting detection algorithms are also discussed. Requirements on data resource and computation by each algorithm are assessed and compared.

STAP is all about obtaining an optimal coherent processing gain of $10log_{10}(MN)$dB with respect to the thermal noise floor, where MN is the dimension of the space-time with M being the number of pulses in a coherent processing interval (CPI) and N the number of antenna elements in azimuth. This potential processing gain may partially or fully disappear if processing is not carried out properly and correctly, or the radar-platform is not calibrated accurately.

Whereas simple Doppler processing leads to a significant signal-to-interference-and-noise ratio (SINR) loss equal to the clutter-noise ratio (CNR) for that Doppler bin, it is desirable to suppress clutter to remove or mitigate this SINR loss. A key processing principle for clutter suppression is space-time processing. Under the detection scenario, a target is supposed to be in the mainlobe direction, different from a sidelobe direction from which clutter having the same Doppler as the target is being received. To achieve clutter suppression in such a scenario, the sufficient and necessary conditions are:

(i) received signals to contain spatial information; and
(ii) a processor to be able to separate spatially different signals.

Satisfaction of the first condition is often achieved by using a linear phased array in the azimuth direction. The realisation of the second condition needs involvement of space-time processing, since unfortunately the clutter covariance matrix is spatial-temporal inseparable.

Classical 'full STAP' using the diagonally-loaded covariance matrix inversion method provides optimal detection for Gaussian clutter but faces a few critical issues. Data and computational expenses are major concerns. Other potential risks include contamination of training data by targets and the training samples not being independent and identically distributed (iid) with respect to the cell under test (CUT).

Mainly to overcome the computational and data expense requirement, quite a significant number of simplified sub-optimal STAP variants have been developed and proposed in the literature over the last 30 years.

The majority of these sub-optimal STAP variants fall in the category of dimension-reduced STAP. While details of these algorithms may vary from one to the other, they share the same or similar concepts and achieve similar results. The most data resource efficient and computation efficient, among other sub-optimal STAP algorithms, is probably the so-called joint-domain localised STAP which adaptively processes a few beams and a few Doppler bins at a time to achieve sub-optimal solutions. With limited support of training data and computation power, this option is probably most attractive.

Representatives of rank-reduced STAP, such as the principle component method and multi-stage Wiener filter aim at achieving data resource efficient which is often critical especially in a heterogeneous clutter environment and for data resource limited cases. However, the realisation of these algorithms demands even more computation than classical STAP at this stage. How to simplify these algorithms to make them computationally efficient needs further research.

Parametric adaptive matched filter and adaptive displaced phase centre antenna utilise the linear autoregressive technique to whiten and decorrelate space-time correlated clutter to simplify the processing. These algorithms are both data resource efficient and computation efficient.

The idea of pseudo-STAP algorithms is to select training samples from historical measurements to ease the problem of lack of sufficient training data and to shift massive calculation of optimal weights to offline. The key to success of these algorithms is the match of the radar and platform parameters between the training data and the data to be processed. Parameter discrepancies (explicitly or implicitly) between training data and data to be processed may incur significant degradation of the performance. Differences in clutter environments between the training data and the data to be processed have ignorable effects on the detection performance.

Knowledge-aided STAP is an architecture rather than an algorithm. Its application with STAP algorithms can result in improvement of detection performance. While its applications are versatile, one of its applications discussed is to assist in selection of training samples particularly in the heterogeneous clutter environment to exclude potentially contaminated or non iid samples using prior knowledge. However, adding the knowledge information system into the processing certainly increases the complexity of the detection problem and requires more computation power to resolve.

There might be no single algorithm that consistently performs best for all scenarios. Detection strategies might be designed and planned in such a way in which various detectors are to be used in different scenarios depends on the computation power and the data resource available to the system. For instance, during a manoeuvre transition period, platform parameters constantly change, and it might not be desirable to use range samples for estimating the weights. Conducting a simple Fourier transform with an appropriate window function to low sidelobe clutter for detection might be a fast and feasible solution. Bearing in mind though, this kind of detection is associated with a SINR loss of CNR varying with Doppler bin to Doppler bin. During a stable and level flying period, if clutter environment is relatively homogeneous and there is sufficient training data, partial STAP or full STAP may be employed depending on the computation power available to the system. If the system is in a routine cruise mission, repeats its surveillance routes, and operators are confident about radar and platform parameters, pseudo-STAP may be used.

Imperfections of radar-platform system may severely deteriorate the overall performance, making the designed gaols not achievable. It is appropriate to make a great effort to perfect the radar-platform including antenna calibration, reduction of mutual coupling and near-field interferences and stability control.

Authors

Dr Yunhan Dong
Electronic Warfare and Radar Division

Dr Yunhan Dong received his Bachelor and Master degrees in the 1980s in China and his PhD in 1995 at UNSW, Australia, all in electrical engineering. He then worked at UNSW from 1995 to 2000, and Optus Telecommunications Inc from 2000 to 2002. He joined DSTO as a Senior Research Scientist in 2002. His research interests are primarily in radar signal and image processing and clutter analysis. Dr Dong was a recipient of both the Postdoctoral Research Fellowships and Research Fellowships from the Australian Research Council.

Contents

Glossary

ADPCA	adaptive displaced phase centre antenna
AEW	airborne early warning
AFRL	Air Force Research Laboratory
AI	Artificial intelligence
CFAR	constant false-alarm rate
CNR	clutter-to-noise ratio
CPI	coherent processing interval
CUT	cell under test
DARPA	Defence Advanced Research Projects Agency
DFT	discrete Fourier transform
DL-CMI	Diagonally-loaded covariance matrix inversion
DoF	degree-of-freedom
DTE	digital terrain elevation
FST	factored space-time
FTS	factored time-space
GIS	Geographic Information System
ICM	internal clutter motion
iid	independent, identically distributed
JDL	joint-domain localisation
KASSPER	knowledge-aided sensor signal processing and expert reasoning
KA-STAP	knowledge-aided STAP
LFM	linear frequency modulation
LULC	land-use land-cover
MCARM	multi-channel airborne radar measurements
MDV	minimum detectable velocity
MIT	moving target indication
MMSE	minimum mean square error
MTS	moving target simulator
MWF	multi-stage Wiener filter
OPP	orthogonal projection processing
PAMF	parametric adaptive matched filter
PRF	pulse repetition frequency
PRI	pulse repetition interval
PSTAP	pre-built STAP
RCS	radar cross-section
RDBMS	rational database management system
RLSTAP	Research Laboratory STAP
RMB rule	Reed-Mallett-Brennan rule
SAR	synthetic aperture radar
SCV	sub-clutter visibility
SINR	signal-to-interference-and-noise ratio
SNR	signal-to-noise ratio
STAP	space-time adaptive processing
ΣΔ-STAP	sum-difference STAP

1. Introduction

One of major missions of an airborne early warning (AEW) radar system is moving target indication (MTI). A moving target can be either airborne or on the ground. An AEW radar must mitigate the otherwise deleterious impact of ground clutter returns and jamming on moving target detection.

In this technical note, we provide a brief overview of various techniques and algorithms proposed to be used by AEW radars for moving target detection. We limit our discussion to an AEW radar that has a side-looking array configuration.

The undesired signals (interferences) for airborne radars normally consist of ground clutter or clutter for short (e.g., radar echoes from the ground), jamming and receiver thermal noise. In this technical note, jamming is not considered in the context of space-time adaptive processing (STAP). In general, point noise jamming signals, if existing, only require space adaptive processing (adaptive beamforming processing) to null and using STAP to reject jamming may not be a computationally efficient choice[1]. Therefore we assume either no jamming or jamming having been excluded by adaptive beamforming processing, and the resulted data to be further processed is jamming-free. Other clutter, such as rain clutter, cloud clutter and so on are also not considered, as this kind of clutter in general behaves like white noise, and its net effect is to add another loss to signal-to-interference-and-noise ratio (SINR). Therefore, the undesired signals (interferences) considered in this technical note are only composed of the ground clutter and the receiver thermal noise. The clutter returns are assumed to be significantly stronger than the thermal noise, and the detection is under a clutter-limited environment.

The probability of detection, P_d, depends on both SINR and the specified probability of false-alarm, P_{fa}. Since there is a monotonic relationship[2] between P_d and SINR for a given P_{fa}, maximising SINR is tantamount to maximising P_d. Therefore, ability to improve SINR is probably a primary criterion for judging a technique or an algorithm. Meanwhile the complexity, the cost (computation and data resource) of the realisation, as well as the reliability should be other criteria.

Since airborne radar is moving, the ground clutter returns exhibit a Doppler spectrum in space (azimuth). Depending on its azimuth direction and radial velocity relative the airborne radar, a specific patch of clutter, has unique and deterministic front-lobe and back-lobe Doppler frequencies. If a moving target in a specific azimuth direction (usually in the mainlobe direction) has the same Doppler frequency as a clutter patch from another direction (usually in sidelobe

---

[1] Having said so, there are differences between using space-only adaptive beamforming to null jamming and STAP to suppress jamming. For the former the detection in that direction may be completely lost as the null processing blinds that direction. The latter however is to suppress the jamming only, and a target in that direction having a high enough signal-to-jamming ratio is still detectable.

[2] Whilst optimal detections have a monotonic relationship, some sub-optimal detections may not. If such is a case, generally other steps are taken by the system to resolve the monotonic performance when such detectors must be used.

directions), STAP is able to separate the target signal from the clutter and hence suppress clutter and improve SINR.

We organise this note as follows. Section 2 briefly reviews STAP and its associated problems. The classic full STAP using the diagonally-loaded covariance matrix inversion (DL-CMI) method is also introduced. Sub-optimal algorithms are then reviewed. Dimension-reduced sub-optimal STAP variants are discussed in Section 3, and the dominant majority of various sub-optimal algorithms can be classified into this category. Section 4 summarises rank-reduced STAP detectors. In general rank-reduced STAP algorithms reduce the requirement on training data but demand more computation power for realisation than full STAP. Parametric adaptive matched filter (PAMF) and adaptive displaced phase centre antenna (ADPCA) are discussed in Section 5. These two algorithms are an alternative to STAP and utilise linear regression technique to whiten and decorrelate space-time correlated signals to simplify the detection problem. They are both data and computational efficient, and associated with only a small detection loss. Discussed in Section 6 is knowledge-aided STAP (KA-STAP) that employs prior knowledge to assist selecting proper training data to improve the performance. Pseudo-STAP algorithms are discussed in Section 7. Utilising historical data and spare computation power, the principle of these algorithms is to shift the data and computation requirements to offline based on a fact that radar and platform may have the same parameters when collecting historical and present data. Commonly discussed STAP is a 2D (azimuth space and time) problem. In fact a phased array is commonly a 2D array. Therefore it is possible to collect data in 3D (azimuth and elevation of space, and time) and processing it in 3D which is discussed in Section 8. Additional processing benefit is achievable using 3D-STAP. Deterioration of detection performance caused by imperfections of radar-platform system including calibration error, near field interferences between radar and platform and so on is discussed in Section 9. Finally Section 10 concludes the note.

2. Space-Time Adaptive Processing

2.1 Optimal Weights of STAP

STAP for radar applications can be traced back to the 1970s (Brennan and Reed 1973). It is now well understood with a large number of publications on this topic available in the literature, including Ward (1994), Klemn (2002; 2004), and Guerci (2003). A recent overview is given by Melvin (2004). A significant number of publications are also cited by these references. If undesired signals obey a multivariate Gaussian distribution, STAP is optimal in the sense of maximising SINR.

In this section we briefly review the model of STAP in the context of a linear airborne side-looking phased array for moving target detection with ground clutter limited conditions. The model also forms a base for reviewing other techniques and algorithms aimed at relaxing the constraints of STAP, i.e., reducing the requirement on the secondary data support and the computational budget.

We assume the phased array discussed in this paper be a linear uniformly spaced 1D array aligned with the flying direction and operated in the side-looking mode. The extension of 1D array to 2D array is later discussed in Section 8. After pulse compression (if employed) and frequency-down conversion, the received snapshot in the baseband is given by,

$$\mathbf{x} = [x_{0,0} \quad \cdots \quad x_{N-1,0} \quad \cdots \quad x_{0,M-1} \quad \cdots \quad x_{N-1,M-1}]^T \tag{1}$$

which is assumed to be multivariate zero mean Gaussian when there is no target present in the data. Element $x_{n,m}$ denotes signal received by channel n and pulse m; the superscript T denotes transpose; N is the total number of channels of the array in azimuth and M is the total number of pulses in a coherent processing interval (CPI). The data sampling rate is assumed to be matched to the bandwidth of pulse compression processing, and that a target occupies only a single range-Doppler bin and the sidelobes of the target are not significant. The optimal weight vector of STAP is (Ward 1994),

$$\mathbf{w}_{opt} = \gamma \mathbf{R}_u^{-1}\mathbf{s} \tag{2}$$

where $\mathbf{R}_u = E\{\mathbf{x}\mathbf{x}^H\}$ is the covariance matrix of the undesired signals; the superscript H denotes Hermitian transpose and γ is an arbitrary scalar ($\gamma = 1$, thereafter). Vector $\mathbf{s}$ denotes the spatial-temporal steering vector of the potential target which is the Kronecker product of the temporal steering vector $\mathbf{s}_t$ and the spatial steering vector $\mathbf{s}_s$, as,

$$\mathbf{s} = \mathbf{s}_t \otimes \mathbf{s}_s \tag{3}$$

$$\mathbf{s}_t = \frac{1}{\sqrt{M}}\left[1 \quad \exp(j2\pi f_d) \quad \cdots \quad \exp(j2\pi(M-1)f_d\right]^T \tag{4}$$

$$\mathbf{s}_s = \frac{1}{\sqrt{N}}\left[1 \quad \exp(j2\pi f_a) \quad \cdots \quad \exp(j2\pi(M-1)f_a\right]^T \tag{5}$$

where f_d and f_a are normalised temporal (Doppler) and special (azimuth) frequencies, respectively.

Assuming the clutter and thermal noise are uncorrelated, the covariance matrix $\mathbf{R}_u$ is a sum of the clutter covariance matrix and the thermal noise (white noise) covariance matrix, as,

$$\mathbf{R}_u = \mathbf{Q} + \sigma^2\mathbf{I} \tag{6}$$

where $\mathbf{Q}$ is the covariance matrix of clutter, σ^2 is the intensity of thermal noise and $\mathbf{I}$ is an identity matrix[3]. The covariance matrix $\mathbf{R}_u$ (mainly the clutter part) is unknown and usually estimated using the maximum likelihood method, by,

$$\hat{\mathbf{R}}_u = \frac{1}{K_l}\sum_{k=1}^{K_l}\mathbf{x}_k\mathbf{x}_k^H + \delta\mathbf{I} \tag{7}$$

---

[3] This is effectively assuming that each antenna element has an independent amplifier and the thermal noise of the amplifier is the dominant noise source. The level of other noise, such as atmospheric noise is much lower than the thermal noise.

where the subscript k denotes range samples. It has been shown that if samples used in estimation are independent and identically distributed (iid) and the number of samples is twofold the dimension of the vector $\mathbf{x}$, i.e., $K_l \geq 2MN$, the resulted SINR loss will be within 3dB, this is also referred to as the RMB rule (Reed *et al.* 1974). The second term is artificially added, known as the diagonal loading to increase the robustness of the estimation and improve the performance. The constant δ is in the order of the system's thermal noise level, and $\mathbf{I}$ is the identity matrix. The diagonal loading approach allows a drastic reduction in the number of samples needed for SINR loss being controlled within 3dB which can be achieved with the number of iid samples to be $K_l \geq 2r_R$, where r_R is the dimension of the clutter subspace, i.e., $r_R = r(Q)$, where $r(\cdot)$ is the rank of a matrix (Li and Stoica 2006; pages 209-210).

To simplify notations, the over-hat for estimated quantities, such as $\hat{\mathbf{R}}_u$ and $\hat{\mathbf{w}}_{opt}$ will be omitted, and such omission should not incur any confusion as any unknowns estimated from data are always the estimated quantities.

The output of the STAP processor is,

$$y = \mathbf{w}_{opt}^H \mathbf{x} \tag{8}$$

The SINR improvement of the STAP processor, $SINR_{stap}$, is defined as the mean power of the output of target signal to the mean power of the output of the undesired signal, as,

$$SINR_{stap} = \frac{\sigma^2 \zeta_t \left|\mathbf{w}_{opt}^H \mathbf{s}\right|^2}{\mathbf{w}_{opt}^H \mathbf{R}_u \mathbf{w}_{opt}} = \sigma^2 \zeta \, \mathbf{w}_{opt}^H \mathbf{s} \tag{9}$$

where ζ_t is the target's single-channel single-pulse signal-to-noise ratio (SNR). The test statistic for a range snapshot $\mathbf{x}$ is thus defined as its output power to the mean power of the undesired signals, as,

$$\Lambda_{opt} = \frac{\left|\mathbf{w}_{opt}^H \mathbf{x}\right|^2}{\mathbf{w}_{opt}^H \mathbf{R}_u \mathbf{w}_{opt}} \tag{10}$$

When Λ_{opt} exceeds a threshold, the presence of a target signal in $\mathbf{x}$ is declared.

The above detection technique, using the diagonally-loaded covariance matrix inversion (DL-CMI) STAP is often referred to as the classical full-rank STAP (or simply the classical STAP). Since it is optimal, often it serves as a benchmark when assessing and evaluating other sub-optimal processors and the associated SINR loss incurred can be calculated at least numerically from either genuine or simulated datasets.

2.2 Architecture of Sample data Selection

Nearly all adaptive algorithms require sample data support to calculate associated parameters adaptively. The sample data is also referred to as secondary data in contrast to the primary data, i.e., the data to be processed for target detection. Primary data and secondary data are mutually exclusive. Understandably, the secondary data are assumed to be target-free. Generally one may use a sliding window of a fixed length to select the secondary data (Ward and Kogon 2004). With the sliding window architecture, the cell under test (CUT) together with a few guard cells, which normally sit in the centre of the window, is excluded from the sliding window. Range samples covered by the window are selected as the secondary data for the CUT, and the window slides as the position of CUT changes. The underlying assumption for this architecture is that the surrounding neighbourhood cells, as the candidates of secondary data, are, if not the iid samples, at least the closest similar samples of the CUT. Since each CUT corresponds to a unique sliding window, it is computationally very expensive. On the other hand, with the fixed window architecture, a signal covariance matrix is estimated from a fixed window, i.e., a block of range samples of the CPI. The same estimates are then applied to another block of cells, rather than a single cell. Obviously the fixed window is much more computationally effective for a given algorithm. Therefore the sliding window seems to be able to provide better results at the expense of huge computational cost. However this was not observed when these two architectures were compared using both simulated RLSTAP datasets and genuine MCARM datasets (Dong 2006). Little gain has been seen using the sliding window against fixed window. This is consistent with an important feature of the clutter covariance matrix: the inverse of the covariance matrix is approximately invariant to changes in clutter intensities received by different range cells (Dong 2005a)[4]. In this technical note, the fixed window is the default architecture when estimating the computational cost as well as examining the performance.

2.3 Critical Issues of STAP

While STAP is optimal (subject to the assumed statistical distributions of data), its implementation over airborne radars faces three critical issues.

First, it requires a significant amount of secondary data samples to support. As mentioned that a number of $K_l \geq 2MN$ or $K_l \geq 2r_R$ iid samples is required to confine SINR loss within 3dB. The rank of clutter covariance matrix is given by (Brennan and Staudaher 1992),

$$r_R = \mathrm{int}\left(N + \beta(M-1)\right) \qquad (11)$$

where β is the ratio of the normalised Doppler frequency to the normalised spatial frequency, which is also referred to as the clutter fold-overs (Ward 1994). The above (*11*) is accurate only if (i) there is no internal clutter motion (ICM), (ii) range is unambiguous and (iii) radar is perfectly calibrated. In reality, because of ICM, involvement of ambiguous range and imperfection of radar calibration, the actual rank of the clutter covariance matrix is often much higher than the theoretical value of (*11*). Therefore, the number of required iid range samples for a good estimate of the covariance matrix can be in an order of hundreds or even thousands for an AEW radar. On the other hand, depending on the range resolution and pulse repetition frequency (PRF), the number of range bins the radar collects in a CPI may only be in an order of hundreds. In addition clutter is often heterogeneous, so range samples are also not iid and nor representative of CUTs. Short of sufficient iid sample data support leads to a degradation of the performance of STAP.

[4] The covariance matrix itself, however, may changes significantly with the selection of different sample cells.

Secondly, STAP requires the inverse of the covariance matrix for construction of the optimal weights. The number of operational counts for matrix inversion is in an order of the cube of the dimension of the matrix. Airborne radars collect a CPI dwell in a fraction of a second, which means that the real-time radar has to process the data at the same rate. The current computer is generally not capable for such a fast response.

Lastly, the sample data is supposed to be target-free. Without prior knowledge, it is difficult in real-time to satisfy this criterion, as it is a chicken-egg problem. If sample data is contaminated, the performance of STAP degrades. For instance, if a highway is included in the secondary data, the moving vehicles in the secondary data will likely mask the detection of other moving targets having the similar radial velocities in the primary data. It has been shown that 10-15dB improvement can be achieved after some prior knowledge is used, and highways have been excluded from the sample data in the processing (Zywicki *et al.* 2003).

Of the above three issues, the second may be mitigated along with the fast development of computer technology. However, the other two remain and even become more critical in conjunction with larger and better airborne radar systems to be deployed in the future. Various proposed sub-optimal STAP variants aim at mitigating the requirement on either sample data support or computer cost or the both while keeping the SINR loss to minimum.

2.4 Principle of Clutter Suppression by STAP

Subsection 2.1 simply states that STAP is optimal. This subsection explains why 2D (space-time, or azimuth-Doppler) STAP outperforms 1D (space-only or time-only) algorithms and provides the maximum clutter suppression for target detection.

Since the relative radial velocity between the ground and airborne radar is azimuth dependent, the associated clutter has a Doppler spectrum. Figure 1 depicts a clutter Doppler spectrum for a case where the radar is operated in a high PRF mode. As shown the radar's unambiguous Doppler region $[-f_{PRF}/2,\ f_{PRF}/2]$ may be divided into three regions:

- Region I, the mainlobe Doppler region. The detection scenario often assumes that the target is in the mainlobe direction, but has a different Doppler frequency from the mainlobe clutter. Therefore the detection in this Doppler region is either not considered, or alternatively the target signal has to be so strong to exceed the mainlobe clutter so that it can be detected.
- Region II, the clutter free region $[-f_{PRF}/2,\ -2v_a/\lambda_0]$ and $[2v_a/\lambda_0,\ f_{PRF}/2]$, where symbols v_a and λ_0 denote platform velocity and radar carrier frequency, respectively. Target signals in this region only encounter competition with thermal noise. The detection is relatively easy, and a standard windowed discrete Fourier transform (DFT) processing is generally sufficient.
- Region III, the sidelobe clutter region, all detection algorithms for airborne radars focus at this region to improve the subclutter visibility (SCV). Algorithms such as STAP are able to fully suppress the clutter in this region if all conditions STAP requires are met, and hence detect target signals embedded in the clutter. As shown in Figure 1, the target embedded in the clutter that would not be detectable without clutter suppression will

becomes detectable once the clutter is suppressed. We explain how STAP is able to suppress clutter in the following paragraphs.

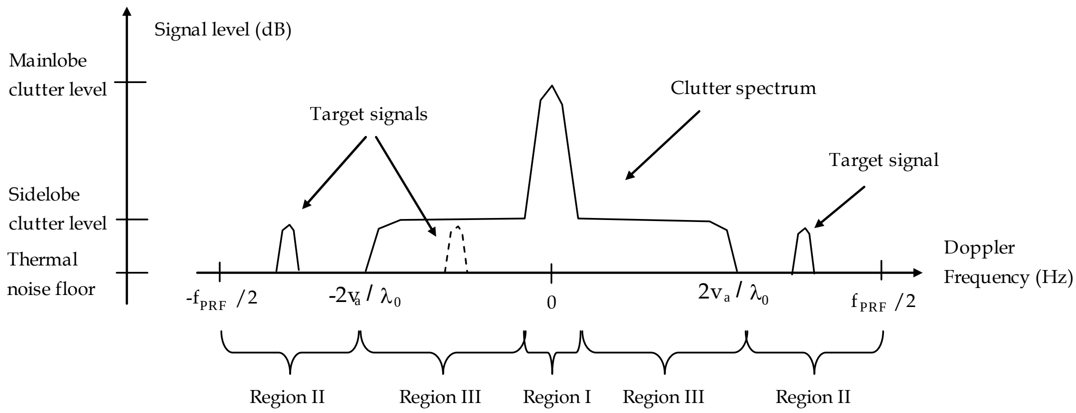

Figure 1: Side-looking high PRF airborne radar clutter Doppler spectrum and its three regions: mainlobe clutter region (region I), clutter-free region (region II) and sidelobe clutter region (region III)

A clutter patch in the nose direction has a maximum radial velocity relative the radar, so the clutter received in this azimuth has the maximum Doppler frequency of $2v_a / \lambda_0$. On the other hand, a clutter patch in the boresight direction (side-looking) does not have any radial velocity relative to the radar, so the clutter received in this azimuth has zero Doppler, and so on. The span of the clutter Doppler, also called clutter ridge (Ward 1994), on the azimuth-Doppler plane is shown in Figure 2. The detection often confined in a specific direction (usually the mainlobe direction) is also shown in the figure. As a consequence, the detection subspace and the clutter subspace are well separated on the azimuth-Doppler plane, and the overlay only happens at the point where the target has the same Doppler as the mainlobe clutter (the detection direction). Therefore, if we can design a processor that suppresses clutter at a specific spatial frequency, then targets having the same Doppler frequency and different spatial frequency will no longer be masked by the clutter and become detectable. Space-time processing is able to suppress the clutter for the whole Doppler band except at the crossover point. It can be seen that the sufficient and necessary conditions for a mechanism to suppress sidelobe clutter are:

1. A target signal having the same Doppler as a patch of clutter has to come from a direction (the detection direction, usual the mainlobe direction) different from that of the clutter patch (sidelobe direction).
2. The above spatial attributes have to be contained in the received signal trains (snapshots), and proper algorithms, such as STAP, must be employed to separate the target signal from the clutter to achieve clutter suppression and detect the target accordingly.

If either of the above two conditions is not satisfied, the detection will suffer from a great SINR loss due to limited clutter suppression.

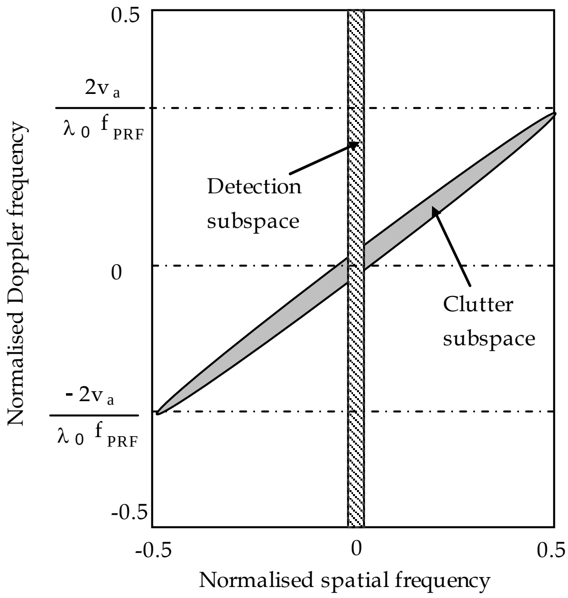

Figure 2: Clutter subspace and detection subspace mapped on the azimuth-Doppler plane

2.5 Spatial-Temporal Inseparable Covariance Matrix

The covariance matrix of interest (*6*) contains two parts, the covariance matrix of the ground clutter and the covariance matrix of the thermal noise. The latter is a spatial-temporal separable matrix, i.e.,

$$\mathbf{C}_n = \sigma^2 \mathbf{I} = \sigma^2 \left(\mathbf{I}_{nt} \otimes \mathbf{I}_{ns} \right) \qquad (12)$$

A space-time covariance matrix $\mathbf{C}$ is called spatial-temporal separable, if it can be expressed by a Kronecker product of $\mathbf{C} = \mathbf{C}_t \otimes \mathbf{C}_s$ (Li *et al.* 2008). For instance, the covariance matrix of point noise jamming, if its aspect and power spectral density are stationary over a CPI, is also spatial-temporal separable, as it can be expressed by a Kronecker product of $\mathbf{C}_j = \mathbf{I}_{jt} \otimes \mathbf{C}_{js}$ (Ward 1994). It can be proven that if a covariance matrix is spatial-temporal separable, the corresponding optimal weights are also separable, and the output of the optimal processor (*8*) can be expressed by (Li *et al.* 2008),

$$\mathbf{y} = \mathbf{w}^H \mathbf{x} = \sum_{n=0}^{N-1} \sum_{m=0}^{M-1} w_n^* w_m x_{nm} \qquad (13)$$

In another words, for a temporal-spatial separable problem, finding an $MN \times 1$ optimal weighting vector can be simplified to finding an $M \times 1$ temporal optimal weighting vector and an $N \times 1$ spatial optimal weighting vector, respectively. The symbol * denotes complex conjugate.

However, the ground clutter is spatially and temporally correlated as both the clutter intensity and Doppler are a function of aspect angle. As a result, the covariance matrix of the ground clutter cannot in general be written as a Kronecker product, and hence it is spatial-temporal inseparable. Since the dominant part of the covariance matrix of interest (Equation (6)) is the ground clutter, therefore, in general the covariance matrix of the ground clutter and thermal noise together is spatial-temporal inseparable. It means that any space-time cascaded processors, such as factored time-space (FTS), factored space-time (FST) and majority of dimension-reduced algorithms discussed in Section 3 are unavoidably associated with some SINR loss. Essentially, all cascaded processors that process data in space-domain and time-domain separately imply the covariance matrix to be spatial-temporal separable which is against the nature of the covariance matrix.

3. Dimension-Reduced STAP Approaches

To overcome problems of full-rank STAP, numerous partially adaptive STAP are proposed in the last three decades, such as those references cited in Ward (1994), Klemm (2004), Melvin (2004) and De Greve et al (2007). Majority of these may be classified into the dimension-reduced STAP, partially adaptive STAP processors aiming to reduce computational cost and sample data support. In general, these processors will inherently incur some SINR loss (as discussed in 2.5). However, it is possible that these partial STAP processors may actually provide better performance with limited secondary data support because of much less estimation loss. This section discusses dimension-reduced methods and leaves rank-reduced approaches in the next section. Most of dimension-reduces algorithms can be classified into four categories by the type of non-adaptive transformation applied by the algorithms (Ward 1994; Himed 2008). Taxonomy of dimension-reduced STAP is shown in Figure 3.

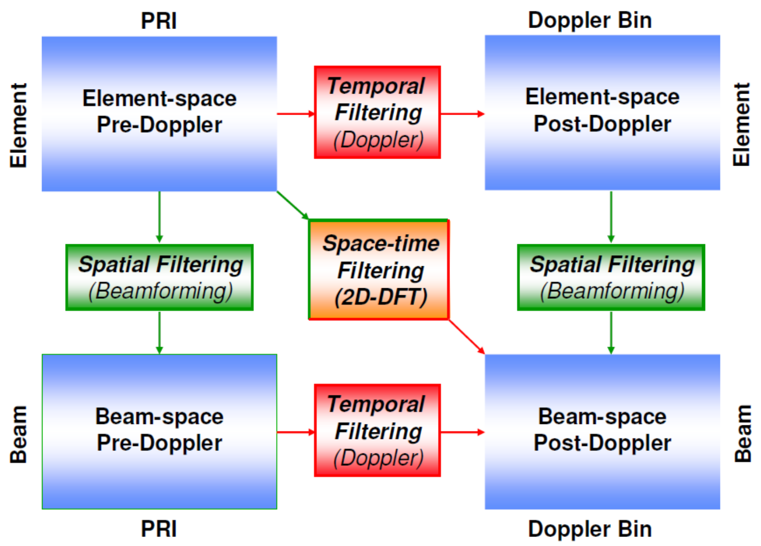

Figure 3: Taxonomy of dimension-reduced STAP algorithms, classified by the type of non-adaptive transformation applied to the CPI data (after Ward, 1994 and Himed, 2008)

The generic architecture of the dimension-reduced STAP is to transform the original $MN \times 1$ data snapshot $\mathbf{x}$ to a new smaller $D \times 1$ vector $\tilde{\mathbf{x}}$ ($D < MN$), and obtain the corresponding sub-optimal weights by (Ward 1994; Melvin 2004),

$$\tilde{\mathbf{w}}_{opt} = \tilde{\mathbf{R}}^{-1}\tilde{s} \qquad (14)$$

where $\tilde{\mathbf{R}} = \frac{1}{K_l}\sum_{k=1}^{K_l}\tilde{\mathbf{x}}_k\tilde{\mathbf{x}}_k^H$, $\tilde{\mathbf{x}} = \mathbf{T}^H\mathbf{x}$ and $\tilde{\mathbf{s}} = \mathbf{T}^H\mathbf{s}$, and $\mathbf{T}$ is the desired dimension-reduced transformation matrix.

3.1 Element-Space Pre-Doppler

Element-space pre-Doppler uses K pulses of the M pulse train (sub-CPI data) at a time to process the data, and reduces the dimension to KN (the value of K is typically 2 or 3). The corresponding transformation matrix is (Ward 1994; Ward and Kogon 2004),

$$\mathbf{T} = \mathbf{J}_p \otimes \mathbf{I}_N \ ; \ \mathbf{J}_p = \begin{bmatrix} \mathbf{0}_{p\times K} \\ \mathbf{I}_K \\ \mathbf{0}_{(M-K-p)\times K} \end{bmatrix} ; \ p = 0,\cdots,M-K \qquad (15)$$

The dimension-reduced data is adaptively processed for each sub-CPI data, followed by the Doppler filtering to obtain the final output. Therefore, element-space pre-Doppler is also said as 'adapt-then-filter'. It retains a full spatial dimension but reduces the temporal dimension by grouping pulses in a CPI. A simplified diagram of element-space pre-Doppler is shown in Figure 4.

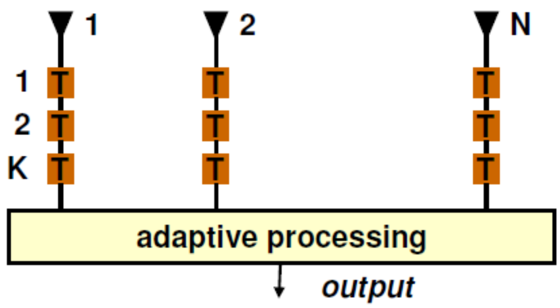

Figure 4: Dimension-reduced Element-space pre-Doppler STAP

3.2 Element-Space Post-Doppler

Whereas element-space pre-Doppler STAP reduces the dimensionality by processing only a few pulses at a time, element-space post-Doppler processes all pulses by Doppler filtering element by element without any adaptation, and then adaptively processes the Doppler-filtered data Doppler bin by Doppler bin. It is also said 'filter then adapt'. The processing diagram is depicted in Figure 5. How adaptive processing part is done may be slightly different and varies from algorithm to algorithm. Other names for this category include post-Doppler adaptive processing, multiwindow post Doppler, factored post-Doppler, factored STAP and so on. The transformation matrix is (Ward 1994; Ward and Kogon 2004),

$$\mathbf{T} = \mathbf{f} \otimes \mathbf{I}_N \tag{16}$$

where $\mathbf{f}$ is one or more coefficient vectors of the Doppler filter bank.

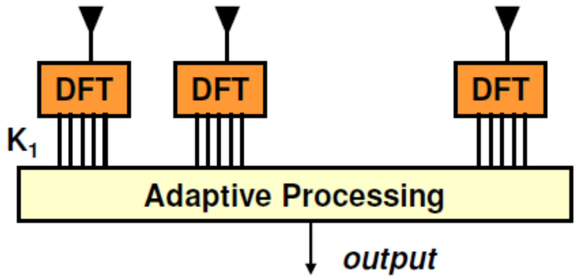

Figure 5: Dimension-reduced element-space post-Doppler STAP

3.3 Beam-Space Pre-Doppler

In the processing of element-space pre-Doppler or post-Doppler, dimensionality reduction is achieved through adaptively processing only a few pulses at a time or adaptively combining a small number of Doppler bins on each element. In many cases, further dimensionality reduction can be achieved by beamforming signals prior to adaptation. Beamforming in this context is a spatial-only operation. In the stage of beam processing, partial of full array elements ($2 \le K_s \le N$) may be selected at a time. Similarly, partial or full pulse train ($2 \le K_t \le M$) may be selected in the transformation matrix. The resulted dimension for the adaptive processing is $K = K_t K_s$. The transformation matrix may be written as (Ward 1994; Ward and Kogon 2004),

$$\mathbf{T} = \mathbf{J} \otimes \tilde{\mathbf{G}} \tag{17}$$

where $\tilde{\mathbf{G}}$ is the desired beamforming matrix. Maximum suppression of clutter is often the primary consideration for the design of the beamforming matrix while using as few beams as possible. Typical beamforming matrices include displaced-beam (displaced phase centre) pre-Doppler and adjacent-beam pre-Doppler (Ward 1994). Therefore, Beam-space pre-Doppler is also said 'displaced phase centre pre-Doppler' and 'adjacent-beam pre-Doppler'.

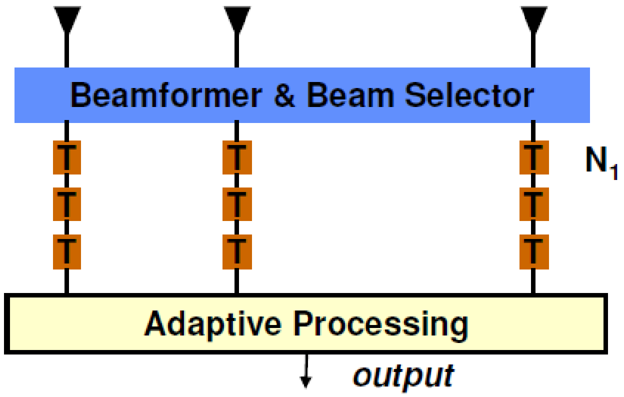

Figure 6: Dimension-reduced beam-space pre-Doppler STAP

3.4 Beam-Space Post-Doppler

A diagram of beam-space post-Doppler is shown in Figure 7. Beamformed data are cascaded by Doppler filtering, the filtered data are adaptively combined to produce final Doppler bin output (Ward and Kogon 2004). This process is repeated for each Doppler bin. Beam-space post-Doppler techniques are a combination of beam-space pre-Doppler and element-space post-Doppler. There are a few variants in this category including displaced-filter beam-space post-Doppler, Adjacent-filter beam-space post-Doppler and so on (Himed 2008).

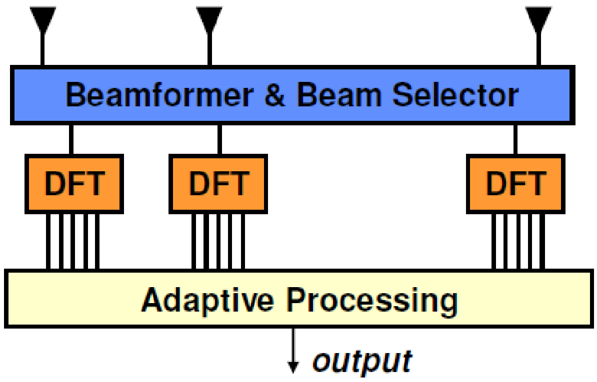

Figure 7: Dimension-reduced beam-space post-Doppler

3.4.1 Sum-Difference STAP

Sum-difference STAP (ΣΔ-STAP) was proposed as an efficient, affordable approach of STAP (Wang *et al.* 2004). It utilises radar's sum channel and difference channel(s) to formulate the optimal weights following the similar procedure of STAP. Because only a few channels are involved, the processing is both computationally and data resource efficient (Wang *et al.* 2004).

In fact, ΣΔ-STAP is a special form of beam-space post-Doppler. The sum and difference channels, whether digitally or analogously formed, are all beamformed channels without adaptivity. These beams are then adaptively processed using adjacent Doppler bins (Wang *et al.* 2004). These channels have little capability separating spatial signals. As a result, we found that ΣΔ-STAP has SINR loss equal to CNR. The SINR loss varies with Doppler, and is equal to the

CNR of sidelobe clutter of that Doppler. Therefore, ΣΔ-STAP can only be described as an optimal processor in the time domain.

3.5 Summary

The above dimension-reduced STAP algorithms provide sub-optimal solutions. The aim of these sub-optimal algorithms is to reduce the requirement of sample data and computation. To achieve this, reducing the dimensionality of adaptation is a key. One of the most data resource efficient algorithms may be the adjacent-filter beam-space post-Doppler processor (Ward 1994), also called joint-domain localised STAP (Wang and Cai 1994). It performs reasonably well even with dimensions of $K_s = 3$ and $K_t = 3$ (Wang and Cai 1994; Ward 1994)[5]. Since the dimensionality can be dramatically reduced, these algorithms are very efficient both computationally and in data resource. The incurred SINR loss is generally no more than a few dB mostly for those Doppler bins close to the Doppler of the mainlobe clutter. Figure 8 shows the performance of the two-stage beam-space post-Doppler processor in comparison with the fully adaptive STAP, using a simulated dataset.

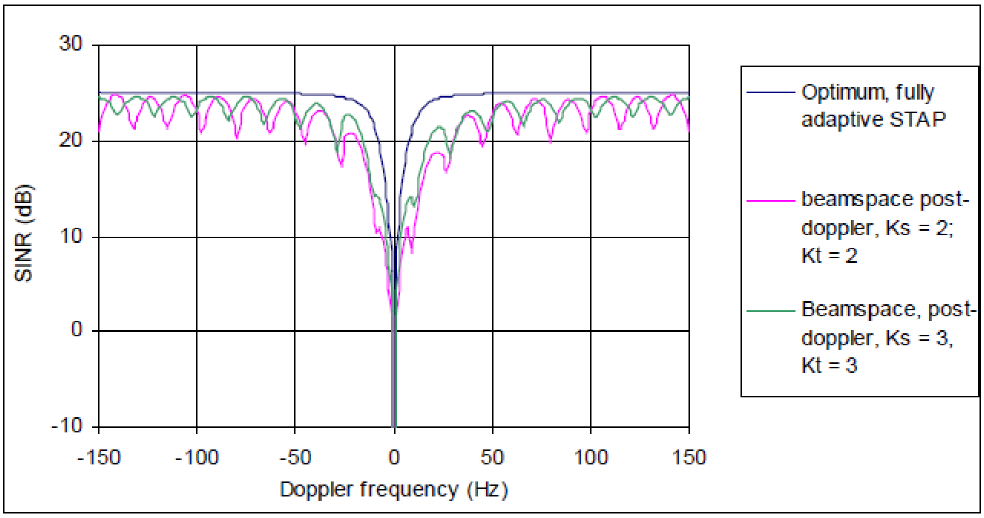

Figure 8: Performance of two-stage beam-space post-Doppler processor in comparison with the fully adaptive STAP, using a simulated dataset)

Using less sample data for adaptation in general is good. However, it may also make the processor to be vulnerable. If all the samples are odd, the resulted statistics from these limited samples are also odd which leads to possible false-alarms or missing detections. On the other hand, such events seldom occur if a large number of samples are used in adaptation.

[5] The original joint-domain localised STAP proposed by Wang and Cai was implemented in the angle-Doppler domain, e.g., the data in the space-time domain was first transformed to the angle-Doppler domain through two-dimensional discrete Fourier transform. A few adjacent beams and Doppler bins were adaptively processed at a time. It was said that the transformation decoupled the degrees-of-freedom necessary for handling clutter suppression, and the clutter subspace in each localised processing region was much smaller than the product of $K_s K_t$.

4. Rank-Reduced STAP Approaches

While dimension-reduced methods apply data-independent transformations to pre-filter data to reduce the number of adaptive degrees of freedom (DoFs), data-dependent transformations are usually used by rank-reduced approaches (Melvin 2004). There are typically two methods in this category. One is the principle component method and the other multi-stage Wiener filter.

4.1 Principle Component Method

The eigen-decomposition of the covariance matrix is written as,

$$\mathbf{R}_u = \sum_{k=1}^{MN} \lambda_k \mathbf{e}_k \mathbf{e}_k^H \qquad (18)$$

where λ_k and $\mathbf{e}_k$ $k = 1, \cdots, MN$, are corresponding eigenvalue and eigenvector, respectively. The inverse of the covariance matrix is,

$$\mathbf{R}_u^{-1} = \sum_{k=1}^{MN} \frac{1}{\lambda_k} \mathbf{e}_k \mathbf{e}_k^H = \frac{1}{\lambda_0} \left(\mathbf{I}_{MN} - \sum_{k=1}^{MN} \frac{\lambda_k - \lambda_0}{\lambda_k} \mathbf{e}_k \mathbf{e}_k^H \right) \qquad (19)$$

where $\lambda_0 = \min\{\lambda_k, k = 1, \cdots, MN\}$, and (*19*) uses the result of $\sum_{k=1}^{MN} \mathbf{e}_k \mathbf{e}_k^H = \mathbf{I}_{MN}$.

The output of the optimal processor (*8*) is,

$$y = \mathbf{w}^H \mathbf{x} = \frac{1}{\lambda_0} \mathbf{s}^H \left(\mathbf{I}_{MN} - \sum_{k=1}^{MN} \frac{\lambda_k - \lambda_0}{\lambda_k} \mathbf{e}_k \mathbf{e}_k^H \right) \mathbf{x} \qquad (20)$$

Because $\frac{\lambda_k - \lambda_0}{\lambda_k} \approx 1$ for $\lambda_k >> \lambda_0$ and $\frac{\lambda_k - \lambda_0}{\lambda_k} \approx 0$ for $\lambda_k \approx \lambda_0$, (*20*) approximates as,

$$y = \mathbf{w}^H \mathbf{x} \approx \frac{1}{\lambda_0} \mathbf{s}^H \left(\mathbf{I}_{MN} - \sum_{k=1}^{J_0} \mathbf{e}_k \mathbf{e}_k^H \right) \mathbf{x} \qquad (21)$$

where J_0 is the number of dominant eigenvalues of the covariance matrix. The above processor is also called the principle component inverse method (Melvin 2004) or simply the PC method (Guerci *et al.* 2000). Since $\mathbf{I} - \sum_{k=1}^{J_0} \mathbf{e}_k \mathbf{e}_k^H$ is a projection matrix orthogonal to the interference subspace, it is also called eigencanceller, or Hung-Turner technique (Li and Stoica 2006, Chapter 4).

Since the PC method only uses the dominant J_0 eigenvectors to process, it requirement on sample data support reduces to $\geq 2J_0$ iid samples to maintain SINR loss within 3dB. In general, eigen-decomposition requires more computational resources than matrix inversion. Therefore, the PC method reduces the demand on secondary data, but does not have any advantages of computing. In fact, as shown by Li and Stoica (Li and Stoica 2006, Chapter 4), the STAP using Diagonal-loading CMI method also only requires range samples to be $\geq 2J_0$.

4.2 Multi-Stage Wiener Filter

The classical Wiener filter is shown in Figure 9. For a jointly complex Gaussian random process $\mathbf{x}_0$, the goal of the Wiener filter is to provide an estimate $\hat{d}_0$ which has the minimum mean square error (MMSE). It is well known, the coefficient vector of the filter is (Goldstein *et al.* 1998),

$$\mathbf{w} = \mathbf{R}_{\mathbf{x}_0}^{-1}\mathbf{r}_{\mathbf{x}_0 d_0} \tag{22}$$

where $\mathbf{R}_{\mathbf{x}_0}$ is the covariance matrix of $\mathbf{x}_0$, i.e., $\mathbf{R}_{\mathbf{x}_0} = E\{\mathbf{x}_0\mathbf{x}_0^H\}$ and $\mathbf{r}_{\mathbf{x}_0 d_0}$ is the cross-correlation of $\mathbf{x}_0$ and d_0, i.e., $\mathbf{r}_{\mathbf{x}_0 d_0} = E\{\mathbf{x}_0 d_0^*\}$.

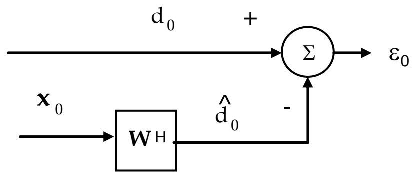

Figure 9: The classical Wiener filter

To derive the multi-stage Wiener filter (MWF), we note that a linear transform of the observation data by a full-rank, non-singular matrix prior to the Wiener filtering does not modify the MMSE. This may be shown in the following. Let $\mathbf{x}_0$ be a MN-dimensional jointly complex Gaussian process with zero means, and consider a non-singular matrix $\mathbf{T}$ which transforms $\mathbf{x}_0$ to $\mathbf{u}$,

$$\mathbf{u} = \mathbf{T}\mathbf{x}_0 \tag{23}$$

The covariance matrix of $\mathbf{u}$ is $\mathbf{R}_u = \mathbf{T}\mathbf{R}_{\mathbf{x}_0}\mathbf{T}^H$. Similarly, the steering vector $\mathbf{s}$ is transformed to $\mathbf{v} = \mathbf{T}\mathbf{s}$. For the new measurement $\mathbf{u}$ with the steering vector $\mathbf{v}$, its optimal output is,

$$y = \left(\mathbf{R}_u^{-1}\mathbf{v}\right)^H \mathbf{u} = \left[\left(\mathbf{T}\mathbf{R}_{\mathbf{x}_0}\mathbf{T}^H\right)^{-1}\mathbf{T}\mathbf{s}\right]^H \mathbf{T}\mathbf{x} = \left(\mathbf{R}_{\mathbf{x}0}^{-1}\mathbf{s}\right)^H \mathbf{x} \tag{24}$$

which is identical to the output of the optimal processor for the measurement $\mathbf{x}_0$ with the steering vector $\mathbf{s}$.

Consider a particular non-singular operator $\mathbf{T}$ with a structure of,

$$\mathbf{T} = \begin{bmatrix} \mathbf{h}_1^H \\ \mathbf{B}_1 \end{bmatrix} \tag{25}$$

where $\mathbf{h}_1$ is the normalised cross-correlation vector, a unit vector in the direction of $\mathbf{r}_{\mathbf{x}_0 d_0}$, given by,

$$\mathbf{h}_1 = \frac{\mathbf{r}_{\mathbf{x}_0 d_0}}{\sqrt{\mathbf{r}^H_{\mathbf{x}_0 d_0}\mathbf{r}_{\mathbf{x}_0 d_0}}} \tag{26}$$

Matrix $\mathbf{B}_1$ is an $(MN-1)\times MN$ operator which spans the nullspace of $\mathbf{r}_{\mathbf{x}_0 d_0}$, such that $\mathbf{B}_1\mathbf{h}_1 = \mathbf{0}$, and has a rank of $MN-1$.

The dimension of $\mathbf{x}_1$, after the transform, as shown in Figure 10, reduces to $MN-1$. The corresponding Wiener filter coefficient vector $\mathbf{w}_1$ may be determined by estimating a $(MN-1)\times(MN-1)$ covariance matrix. Hence the rank of the problem reduces by 1 through a two-stage Wiener filter. Recursively applying this principle and structuring a multi-stage Wiener filter, we can significantly reduce the rank of the problem. A multi-stage Wiener filter is depicted in Figure 11, with the null conditions of $\mathbf{Bs}=0$, $\mathbf{B}_1\mathbf{h}_1=0$, …, $\mathbf{B}_i\mathbf{h}_i=0$.

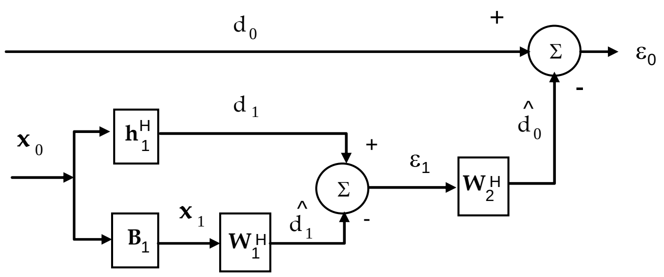

Figure 10: Two-stage Wiener filter

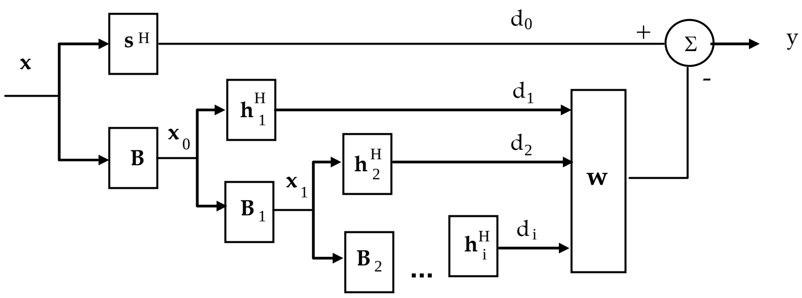

Figure 11: Multi-stage Wiener filter

Since the rank of the original problem can be significantly reduced by the multi-stage Wiener filter, the corresponding requirement on the number of samples to support also greatly reduces. Guerci et al (2000) claim that MWF can yield even a lower interference subspace than the PC method. According to their numerical test on genuine clutter datasets collected by the DARPA Mountain Top radar, the clutter rank generated by the PC method was 29 compared to 15 resulted by MWF. They also indicate that another advantage of MWF over the PC approach is its robustness to errors in estimating the rank of the interference subspace. PC may suffer a significant degradation, compared to MWF, in performance if the interference subspace rank is underestimated.

This section briefly reviews two approaches of rank-reduced STAP, i.e., MWF and PC. In general, the rank reduction is data-dependent whereas the dimension-reduction reviewed in Section 3 is generally data-independent reduction. Another important factor to notice is that the two approaches introduced in this section generally demand more computation to complete than full STAP. At the moment, these two approaches are only data-resource efficient but not computational efficient. How to implement these algorithms effectively in computation deserves further investigation.

Some authors (Melvin 2004) tend to also classify PAMF introduced in Section 5 in the category of rank-reduced STAP. It is true that the rank reduction of PAMF and ADPCA is data-dependent. However, both of them are not only data-resource efficient but also computation efficient. Therefore, PAMF and ADPCA are reviewed in a separate section in this note.

5. Parametric Adaptive Matched Filter and Adaptive Displaced Phase Centre Antenna

5.1 Parametric Adaptive Matched Filter (PAMF)

Parametric adaptive matched filter (PAMF) for airborne radar was proposed by researchers sponsored by the Air Force Research Laboratory (AFRL) (Roman *et al.* 2000). The modified version of PAMF is also available (Dong 2006). Theoretically the maximum coherent processing gain STAP can achieve is $10\log_{10}(MN)$, and MN is referred to as the dimension of the algorithm. PAMF has a dimension of $(M-p)N$, where p is the order of the PAMF, and typically has a value of 3–5. Therefore PAMF has a dimension loss, i.e., its maximum achievable coherent processing gain is slightly lower, so is the associated Doppler resolution. The modified version of PAMF (Dong 2006) does not have any dimension loss, and it is especially beneficial when M is small. Different from STAP, PAMF employs the linear autoregressive (AR) processing to whiten and decorrelate the space-time correlated clutter, and the calculation of the adaptive parameters for the AR processing is much more effective. In consequence, PAMF has two advantages over STAP: it is much more computationally effective and requires much less sample data to support. The equivalent covariance matrix for PAMF has a dimension of pN that is significantly smaller than MN, (usually $M >> p$). PAMF uses averaging processing in both the fast-time domain (average over range bins) and the slow-time domain (averaging over pulses). Hence firstly PAMF has a reduced size of the covariance matrix and secondly is does more averaging manipulations with sample data. Therefore, PAMF is much more data source efficient and requires much less secondary data to support compared to STAP. In contrast, STAP only utilises the averaging processing in the fast-time domain to estimate its covariance matrix.

Mathematically, PAMF assumes that the array measurements $\mathbf{x}(m) \in C^{N\times 1}$, $m = p, p+1, \cdots M-1$, by the current pulse m can be estimated using the previous p measurements, $\mathbf{x}(m-k)$, $k = 1, \cdots, p$, as,

$$\hat{\boldsymbol{\varepsilon}}(m) = \mathbf{x}(m) - \hat{\mathbf{x}}(m) = \mathbf{x}(m) - \sum_{k=1}^{p} \mathbf{A}^H(k)\mathbf{x}(m-k) \qquad m = p, \cdots, M-1 \tag{27}$$

The AR processing is used to adaptively estimate the filter parameters $\mathbf{A}(k)$, $k = 1, \cdots, p$. Obviously, this processing requires a stationary linear system, so, $\mathbf{A}(k)$ can be linearly regressed and independent of pulse m.

Let us further investigate differences between STAP and PAMF. Since PAMF also utilises the averaging processing in the slow-time domain, it naturally requires the pulses in a CPI have to be stable and identical which however can be satisfied in general. A structure of the covariance matrix of undesired signals $\mathbf{R}_u$ is shown in Figure 12 where each element is a $N \times N$ block submatrix, and a case of $M = 6$ and $p = 2$ are shown. STAP uses the whole covariance matrix to calculate the optimal weights whereas PAMF only selects those elements in the rectangular frames to estimate the weights, and discards the remaining. PAMF also carries out averaging processing over the frames, assuming their identification. Obviously, if the covariance matrix is perfectly known, the partially discard by the PAMF would result in some SINR loss. However, in reality, the estimated covariance matrix may not be so accurate, and making use of the whole by STAP may lead to some distortions and even cause some SINR loss. On the other hand, the partial discard by PAMF may introduce little SINR loss.

According to our testing using RLSTAP datasets and MCARM datasets, the performance of PAMF is almost identical to STAP, except a possible few dB loss for detection at Doppler frequencies close to the Doppler of the mainlobe clutter (Dong 2006). A number of $2pN$ range samples in general are sufficient to support PAMF. The computational cost is only a small portion of what STAP requires. If the sliding window architecture is used in processing, the computational cost of PAMF expressed as percentages of the cost of STAP is shown in Figure 13. It can be seen that the percentage varies as a function of element number N, pulse number M and number of CUT to be processed. In some cases, the computational savings can be >90%.

$$\begin{pmatrix}
\mathbf{R}_u(0,0) & \mathbf{R}_u(0,1) & \mathbf{R}_u(0,2) & \mathbf{R}_u(0,3) & \mathbf{R}_u(0,4) & \mathbf{R}_u(0,5) \\
\mathbf{R}_u(1,0) & \mathbf{R}_u(1,1) & \mathbf{R}_u(1,2) & \mathbf{R}_u(1,3) & \mathbf{R}_u(1,4) & \mathbf{R}_u(1,5) \\
\mathbf{R}_u(2,0) & \mathbf{R}_u(2,1) & \mathbf{R}_u(2,2) & \mathbf{R}_u(2,3) & \mathbf{R}_u(2,4) & \mathbf{R}_u(2,5) \\
\mathbf{R}_u(3,0) & \mathbf{R}_u(3,1) & \mathbf{R}_u(3,2) & \mathbf{R}_u(3,3) & \mathbf{R}_u(3,4) & \mathbf{R}_u(3,5) \\
\mathbf{R}_u(4,0) & \mathbf{R}_u(4,1) & \mathbf{R}_u(4,2) & \mathbf{R}_u(4,3) & \mathbf{R}_u(4,4) & \mathbf{R}_u(4,5) \\
\mathbf{R}_u(5,0) & \mathbf{R}_u(5,1) & \mathbf{R}_u(5,2) & \mathbf{R}_u(5,3) & \mathbf{R}_u(5,4) & \mathbf{R}_u(5,5)
\end{pmatrix}$$

Figure 12: Structure of the covariance matrix. Elements in the rectangular frames are used in PAMF processing, and those outside the frames are discarded and not used.

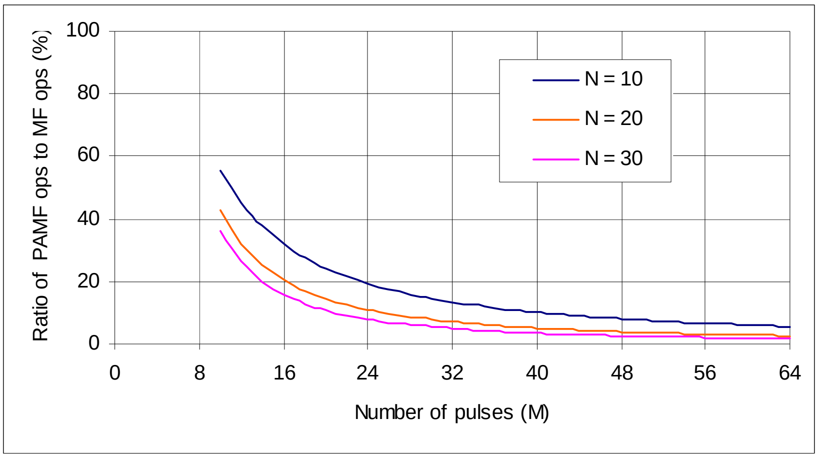

(a)

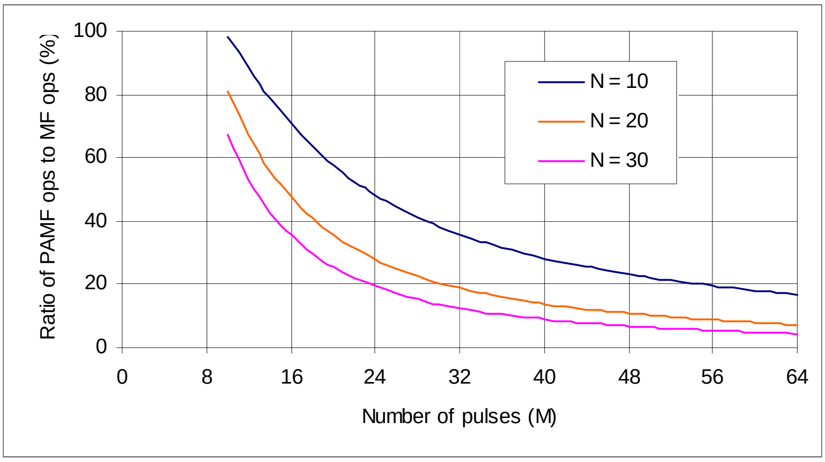

(b)

Figure 13: Computational cost of PAMF expressed as percentage of the cost of STAP using the sliding window processing architecture for processing of (a) 100 range bins and (b) 500 range bins

5.2 Adaptive Displaced Phase Centre Antenna

Displaced phase centre antenna (PDCA) processing is a technique for countering the platform motion induced clutter spectrum spread. The basic concept is to make the antenna appear stationary even though the platform is moving forward by electronically shifting the receive aperture backwards during the operation. For airborne radar, a typical way to achieve this is to adjust the radar PRF according to the platform velocity so that the first, second, etc antenna elements at the current pulse effectively move to, respectively, the exact positions of the second, third, etc antenna elements at the previous pulse, and so on. This often refers to the DPCA condition. In practice, even if the DPCA condition is satisfied, the clutter cancellation is still limited, due to various disturbances introduced by the radar, platform, and clutter environment (ICM, for instance) and the bandwidth of two pulses. To overcome these issues, the so called adaptive DPCA concept has been introduced. The conventional ADPCA algorithm proposed by Blum et al. (1996) which has been widely re-introduced by airborne radar textbooks (Klemm 2002, Chapter 7; Guerci 2003, Chapter 5), unfortunately has technical flaws, and is not an optimal processor and consequently could have significant SINR loss (Dong 2007). Instead

Dong (2007) proposed a new version of ADPCA, it is in fact a combination of AR processing and DPCA technique. From the algorithm point of view, it is equivalent to the case of PAMF with $p = 1$. However, since it also employs the DPCA principle, its performance can match with a higher filtering order PAMF ($p = 3 \sim 5$). As explained, the lower order PAMF also means less computation and less sample data required.

It has been found that the proposed ADPCA (Dong 2007) performs nearly as well as STAP, suffering at most a few dB of processing gain loss in the vicinity of the Doppler of the mainlobe clutter. However if there are insufficient clutter samples to accurately estimate the covariance matrix, the performance of STAP is severely degraded whereas the proposed ADPCA still performs as well as before. Mathematically STAP requires estimation of a covariance matrix whose size is the product of the number of antenna elements and the number of pulses in a CPI. On the other hand, the proposed ADPCA estimates its parameters by the use of a covariance matrix whose size is the number of antenna elements minus one. In addition, in estimating parameters, STAP uses averaging processing only in the fast-time domain, whereas ADPCA utilises averaging processing in both the fast-time and the slow-time domains. These two differences make the proposed ADPCA more robust and require far less sample data. In general, the parameters of the ADPCA can be satisfactorily estimated once the number of range samples is equal to or greater than twice the number of antenna elements. The Blum ADPCA, on the other hand, is not an optimum processor and its performance usually is poor and suffers significantly especially when the target's Doppler is close to that of the mainlobe clutter. To appreciate the proposed ADPCA with reduced sample data, Figure 14 and Figure 15 compare detection performances of STAP, Blum's ADPCA and the proposed ADPCA. It clearly shows that with reduced sample data, both STAP and Blum's ADPCA cannot sustain their performance level, whereas the proposed ADPCA still robustly can.

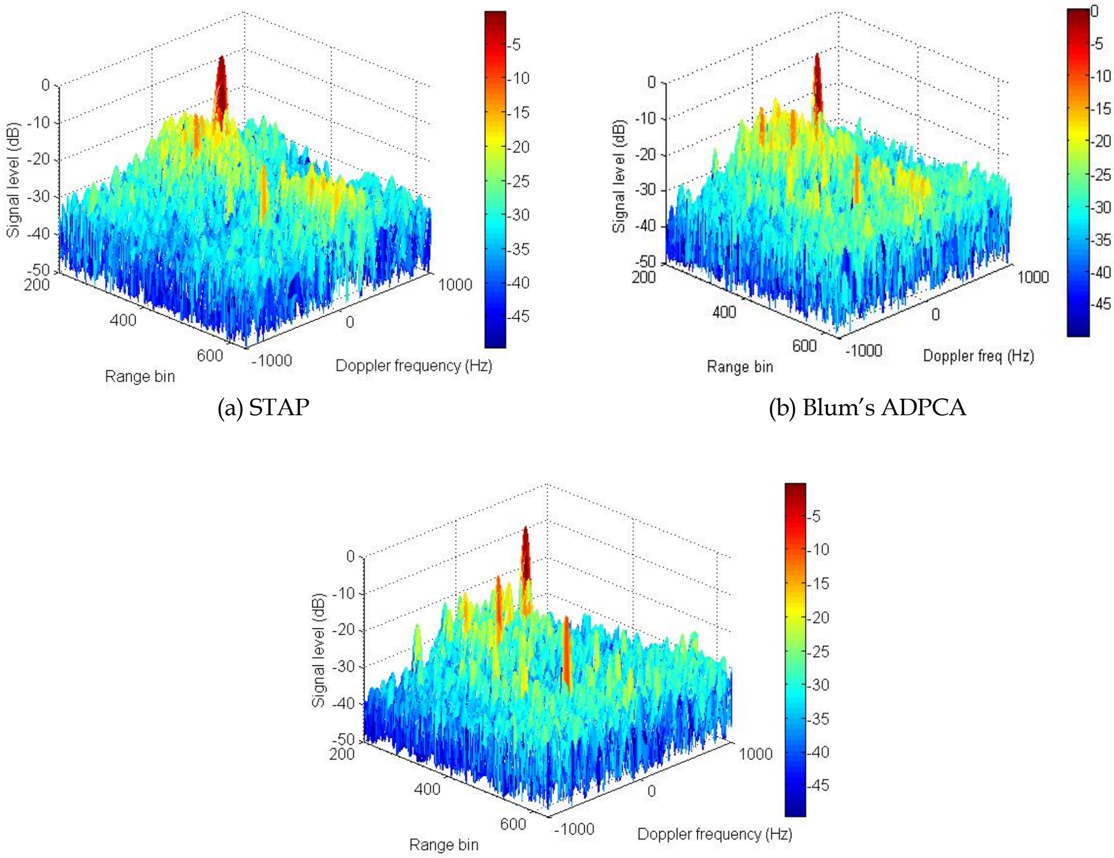

(a) STAP

(b) Blum's ADPCA

(b) Proposed ADPCA

Figure 14: Detection results of MCARM data by the use of (a) STAP, (b) Blum's ADPCA and (c) proposed ADPCA using 400 range samples. The stronger target in range bin 299 is a genuine moving target, and weaker target in range bin 500 is the injected artificial moving target. There are notably higher mainlobe clutter residuals for STAP and Blum's ADPCA.

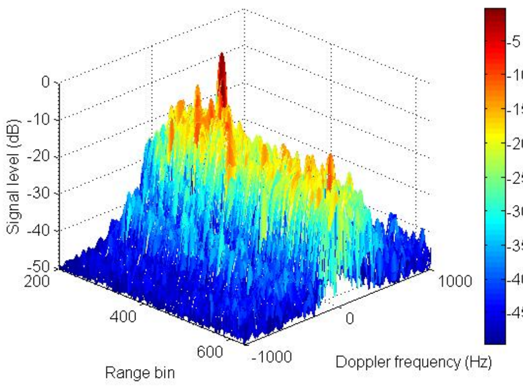

(a) STAP

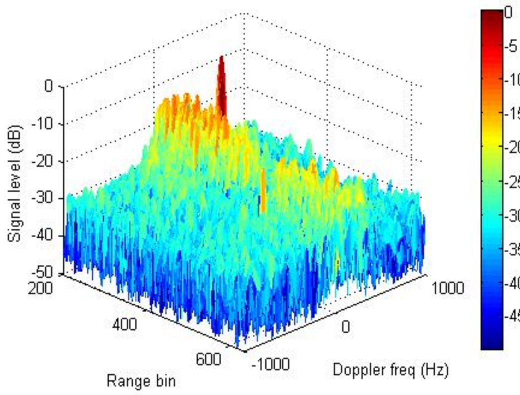

(b) Blum's ADPCA

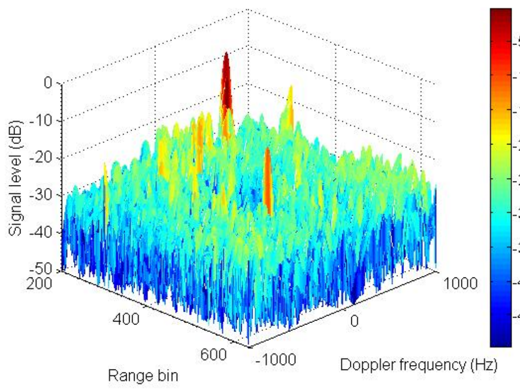

(c) Proposed ADPCA

Figure 15: Detection results of MCARM data by the use of (a) STAP, (b) Blum's ADPCA and (c) proposed ADPCA using 21 range samples. With such reduced sample data, STAP and Blum's ADPCA cannot retain their performance level whereas the proposed ADPCA suffers little compared to Figure 14.

The second advantage of the proposed ADPCA is the savings of computation. The operational counts required for the proposed ADPCA has been estimated (Dong 2007). In general, it only requires 5-10% of the computation of STAP. In addition, since most of the computation for the ADPCA algorithm is linear transforms, parallel processing and/or hardware realisation can be easily implemented. In contrast, the dominant calculation of the STAP algorithm is the inversion of the covariance matrix which is not a linear transform limiting the application of parallel processing. In this sense, computational savings of the ADPCA algorithm is even greater than the simple operational counts estimation and comparison.

We need to point out that ADPCA is inherently a dimensionality-loss process. Both the number of effective antenna elements and the number of effective pulses in a CPI are reduced by one. Therefore, theoretically the maximum coherent processing gain it can achieve is $10\log_{10}[(M-1)(N-1)]$ dB compared to the gain of $10\log_{10}(MN)$ dB for STAP. In addition, a few dB loss for detection at Doppler frequencies close to the Doppler of the mainlobe clutter is also possible.

6. Knowledge-Aided STAP and Metacognitive Radar

Discussing development of STAP for airborne radar, one needs to mention knowledge-based or knowledge-aided STAP (KA-STAP), initially proposed by researches of DARPA (Guerci 2004). KA-STAP is a key element of the knowledge-Aided Sensor Signal Processing and Expert Reasoning (KASSPER) program of DARPA. Typical STAP operating environments are heterogeneous, violating the requirement of the training data to be iid. A key issue is how to select representative candidates in the secondary data for estimation of the covariance matrix to improve performance. The covariance matrix estimation error leads to filter mismatch and could result in enormous SINR loss in some cases. KA-STAP utilises other resources to provide additional prior knowledge to enhance radar's performance in complex, heterogeneous clutter environments (Guerci 2002; Melvin *et al.* 1998; Zywicki *et al.* 2003). Typical aiding knowledge provided to radar includes synthetic aperture radar (SAR) imagery to provide clutter maps; land cover and land usage (LCLU), site information and digital terrain elevation (DTE) data to provide heterogeneous and site-specific information to assist sorting training data. In this application KA-STAP utilises a priori information and implements a knowledge-aided front-end signal processing window to smartly select secondary data samples best matching to the CUT to overcome or mitigate the problem of heterogeneous clutter. The resultant performance is therefore expected to be improved over the same STAP algorithm with blind selection of secondary data samples.

A knowledge-aided framework proposed in (Zywicki *et al.* 2003) is shown in Figure 16. The front-end consists of knowledge resources and scenario-specific information feeding into a Geographic Information System (GIS) and Rational Database Management System (RDBMS). The front-end is connected to the signal processor in a feedback mechanism allowing multiple pass training and optimisation of the STAP processor for the scenario specific environment. The method of training, algorithm selection and inclusion of database resources is determined through case-based reasoning. This allows an expert reasoning system to be developed over time that takes advantage of benchmarked performance of STAP strategies in various representative environments.

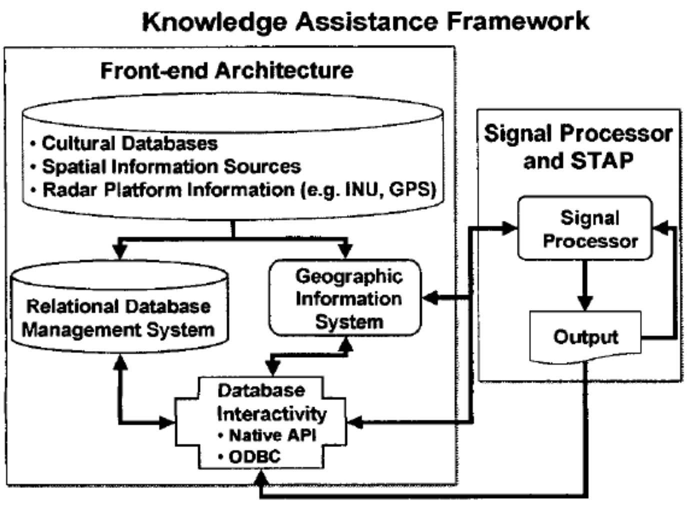

Figure 16: Framework of KA-STAP for implementation of a priori information in a front-end architecture (after Zywicki et al. 2003)

Zywicki et al. (2003) present two applications of KA-STAP in processing MCARM data. In the first, LULC and other information are used to remove range bins of a major highway from the training data. Since the removal of these range bins also removes ground moving vehicles, thereby improving minimum detectable velocity (MDV). In this example the intelligent training offers 10 to 20dB SINR improvement for those Doppler bins having the similar Doppler frequencies of the ground moving targets. SAR imagery is utilised in the second example to exclude extreme clutter discrete (large buildings, power towers etc). Discrete large returns tend to be under-nulled in the typical STAP implementation, leading to either high false alarms or low detections. After the removal of the discrete from the training data, false alarms are reduced, which in turn, improves the detection.

In general, applications of KA-STAP are not limited only to the selection of training data. Other applications, such as selections of waveform, PRF, CPI, power level and so on can also be included in the category of KA-STAP.

AFRL has conducted and sponsored a similar research program known as Airborne Intelligence Radar System (AIRS) (Capraro and Wicks 2010; Capraro *et al.* 2006; Capraro and Wicks 2004). Futuristic advanced intelligent radar systems will cooperatively perform signal and data processing within and between sensors and communications systems as shown in Figure 17. If a radar system is built using knowledge based techniques then there exists intelligence to control signal and data processing. The processors shown in the figure operate independently and cooperatively. For instance, radar's frequency, waveform, antenna configuration and so on are controlled by the block of configuration. Clutter map and environmental information such as weather and jammer locations are provided. Flight profiles are preloaded and updated continuously from the platform's navigation system. Information of intelligence is also available from intelligence community before and during a mission. The difference between knowledge-aided radar and intelligent radar systems is that the latter is supposed to learn over time by monitoring the performance of different algorithms over various environments.

The merging of artificial intelligence (AI) and radar signal processing is an area that AFRL has been pursuing for many years. As each area (AI and signal processing) advances, larger benefits will be obtainable by integrating AI into signal and data processing. Metacognition refers to the active control over the cognitive processes one uses to understand how they learn. Metacognitive radar or AI radar is said to be the next level of the knowledge-based radar (Capraro and Wicks 2010). It means that metacognitive radar should be built in such a way that it can its performance by learning new facts, rules and strategies especially under dynamic environments.

Similarly, Haykin proposed cognitive radar as the next generation of radar in recent years (Haykin 2006). The cognitive radar is motivated by how human's brain works, and it at least has the four essential processes (Haykin 2010):

1. Perception in receiver, which is followed by action in the transmitter through feedback from the receiver to the transmitter to maximise information gain;
2. Memory, which is configured to identify consequences of selections/actions taken by the radar receiver and the transmitter;
3. Attention, the purpose of which is to prioritise the allocation of available resources; and

4. Intelligence which manifests itself in decision-making for selecting intelligent choices in the face of environmental uncertainties.

The cognitive radar is still in the stage of high level concept debating at the moment. The community is eager to see such a radar to be constructed in the future.

It is understood, KASSPER, metagonitive radar or cognitive radar is in general an architecture that cooperates and integrates sensors, processors, data and information resources as well as intelligence to achieve an overall better performance. On the other hand, algorithms, such as STAP and its variants, are essentials for processors. Therefore, any advanced radar needs the support of basic algorithms in fulfilment of the relevant tasks at the processor level.

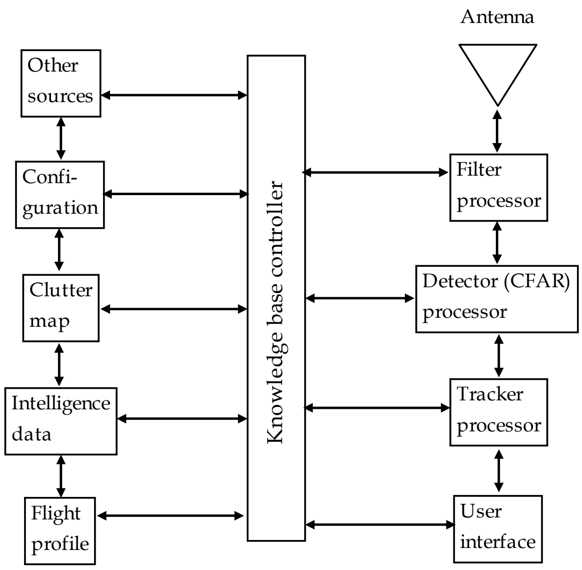

Figure 17: Airborne intelligent radar system (after Capraro and Wicks, 2010)

7. Pseudo-STAP Variants

As discussed, STAP is optimal but faces three critical issues: (i) limited secondary data; (ii) limited computational budget and (iii) contamination of secondary data. Various dimension-reduced and rank-reduced STAP variants aim at mitigating requirement of either sample data or computational cost or the both. KA-STAP employs known information to select best training data to match CUT and reduce or exclude contamination. Page et al (2004) suggested to use the past CPI data to construct the covariance matrix, which otherwise is difficult to be estimated accurately due to lack of homogenous range data in the current CPI.

The clutter covariance matrix is collectively determined by (i) properties of clutter such as reflectivity, ICM and so on, and (ii) radar and platform parameters including illumination geometry, array configuration, wavelength, PRF, resolution, velocity, etc. If an AEW radar is in a cruise mode, radar and platform parameters may remain unchanged in a short period when collecting a number of CPI datasets. In this situation, data collected by previous CPIs may be used as candidates of the secondary data and the resulted weights are applied to the current measurement to provide optimal or near-optimal output. In this architecture, previous measurements are used to generate optimal or near-optimal weights. Hence it may be referred to as pseudo-STAP. Since the radar and platform parameters are generally well controllable, the previous and historical CPI data may refer to data collected seconds, minutes, hours, days or even months ago. General architecture of pseudo-STAP is shown in Figure 18. This architecture mitigates all three critical issues of STAP mentioned above. First, numerous historical CPI data provides sufficient sample data. Secondly, the computation of the weights is shift to offline and does not compete with the current processing. Lastly, the selection of the secondary data can be conducted with assistance of other means to ensue sample data to be contamination-free.

Under this pseudo-STAP architecture, we in particular introduce two techniques, pre-built STAP (PSTAP) and eigencanceller.

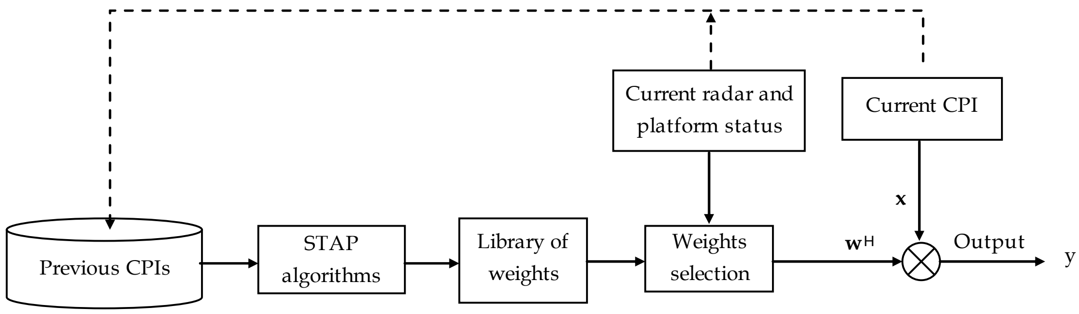

Figure 18: Architecture of pseudo-STAP

7.1 Pre-Built STAP

It has been found that the inverse of the covariance matrix of ground clutter is approximately invariant with respect to the changes in the clutter environment provided that radar and platform parameters remain unchanged (Dong 2005a). In general, changes in the clutter environment often results in changes in the clutter covariance matrix. However, STAP only requires the information of the inverse of the covariance matrix (but not the covariance matrix itself) that is, however, approximately invariant to changes in the clutter environment. As an example, Figure 19 shows two covariance matrices, simulated from two different clutter environments, with the differences caused by the different clutter reflectivity coefficients. In the figure, x-, y- and z-axes stand for row, column and the element's value of the covariance matrix, respectively. Their corresponding inverses, also shown in the figure, however are highly correlated and approximately invariant. No visual differences are found between the two inverses. In fact, a numerical element-to-element analysis for the two inverses results in a correlation coefficient of $r^2 > 0.99$. Details of mathematical proof for the above assertion of the approximately invariant inverse are given in (Dong 2005a).

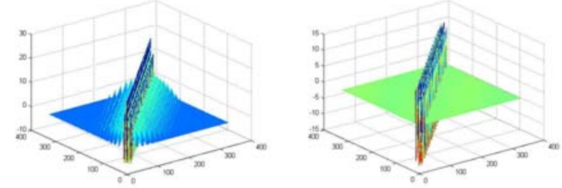

(a) Real part and imaginary part of the covariance matrix of case 1

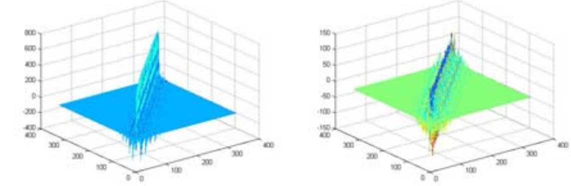

(b) Real part and imaginary part of the inverse of case 1

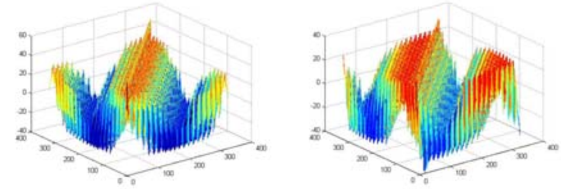

(c) real part and imaginary part of the covariance matrix of case 2

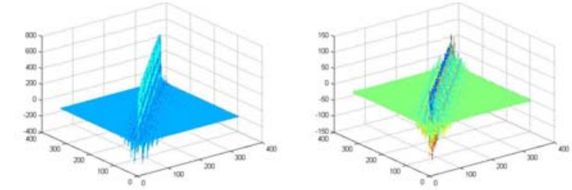

(d) Real part and imaginary part of the inverse of case 2

Figure 19: Significant differences exist in covariance matrices shown in (a) and (c) whereas no differences can be visually found in their corresponding inverses shown in (b) and (d). A numerical element-to-element analysis results in a correlation coefficient of $r^2 > 0.99$ *for the two inverses.*

Based on the assertion, a processor, called pre-built STAP (PSTAP) is proposed (Dong 2005a). Previous CPI data are used as the secondary data for estimation of the covariance matrix and the resulted optimal weights are then directly applied to the current CPI data for target detection. Results of the traditional full-rank STAP are used as benchmarks to gauge the performance of PSTAP. Though more sample data may be available for PSTAP, we used the same number of range samples in both STAP and PSTAP processing in this paper in order to have a fair comparison.

To investigate performance of PSTAP, simulated datasets are generated using the high fidelity airborne simulation software, RLSTAP (Dong 2005b). Figure 20 compares results of STAP and PSTAP using the RLSTAP datasets. The result of STAP here means that the same CPI dataset (dataset #2) is used to estimate its covariance matrix, the weights are then applied to the same dataset for target detection (thought the primary and secondary data are mutually exclusive). On the other hand, the result of PSTAP here means that the inverse of the covariance matrix is estimated from one dataset (dataset #7) and then used to processing the other dataset (dataset #2) for target detection. The clutter environments are different for different datasets (in fact they were the Seattle and Washington DC areas, respectively), but the radar and platform parameters are the same. It can be seen that both STAP and PSTAP perform approximately the same. Details of clutter environments, radar and platform parameters, and how datasets were generated by RLSTAP may be found in (Dong 2005b).

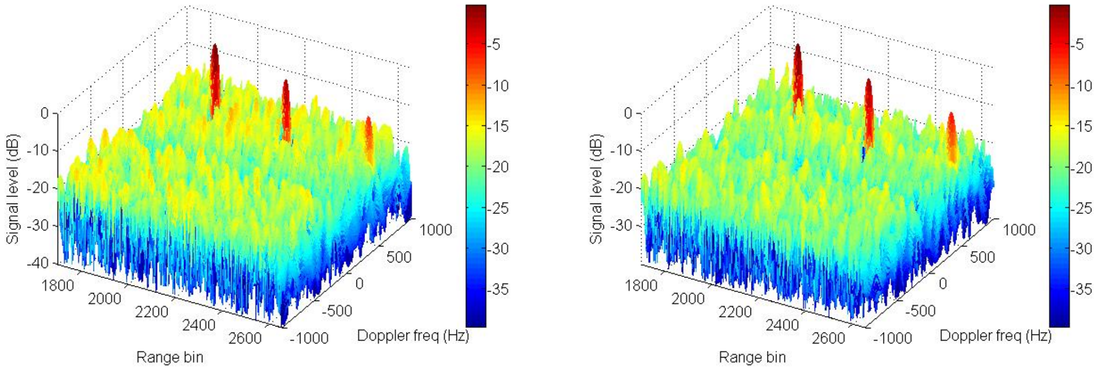

(a) STAP (#2, #2) (b) PSTAP (#7, #2)

Figure 20: Comparison between STAP and PSTAP for detecting three 1m² targets in Dataset #2. PSTAP used the covariance matrix estimated from Dataset #7.

Performances of STAP and PSTAP are also compared using MCARM datasets, as shown in Figure 21. Dataset RE050152 was processed by STAP and PSTAP. For PSTAP another dataset, RE050155, which has the same radar parameters and the nearly same platform parameters, was used for the estimation of the inverse of the covariance matrix. It can be seen that the moving target simulator (MTS) signals in range bin 450 have been observed by both processors. The strong clutter residuals, especially in near range bins resulted from the two processors having a similar level. These strong residuals can be further suppressed if the range effect on clutter returns, i.e., near range has higher clutter returns than far range bins, was considered and removed in the processing. Here the main point to demonstrate is that PSTAP works equally well as STAP, if not better (PSTAP may have more homogeneous samples to estimate the inverse of the covariance matrix, and hence can outperform STAP which may suffers from limited and heterogeneous samples).

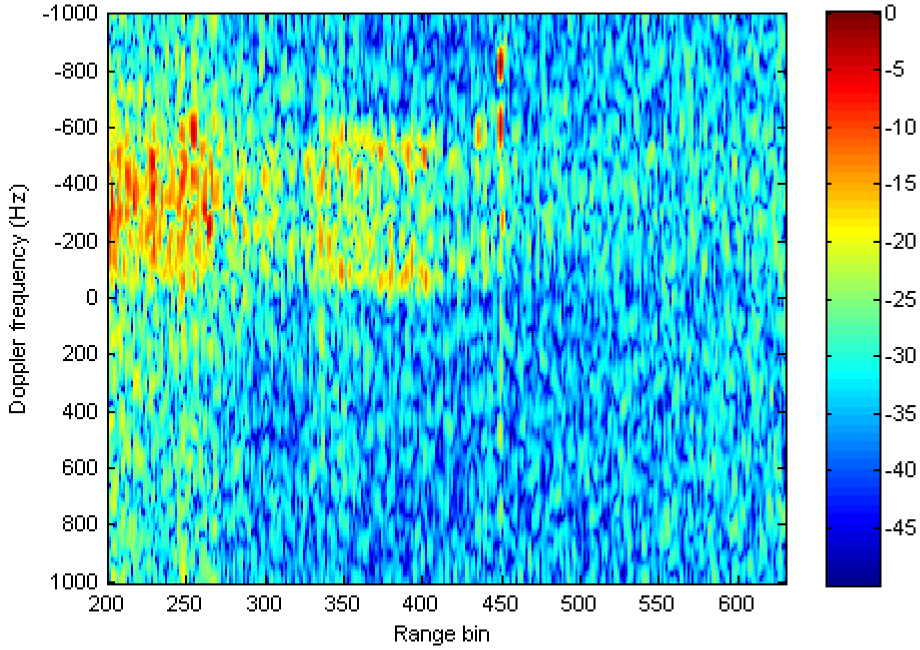

(a) STAP (RE050152)

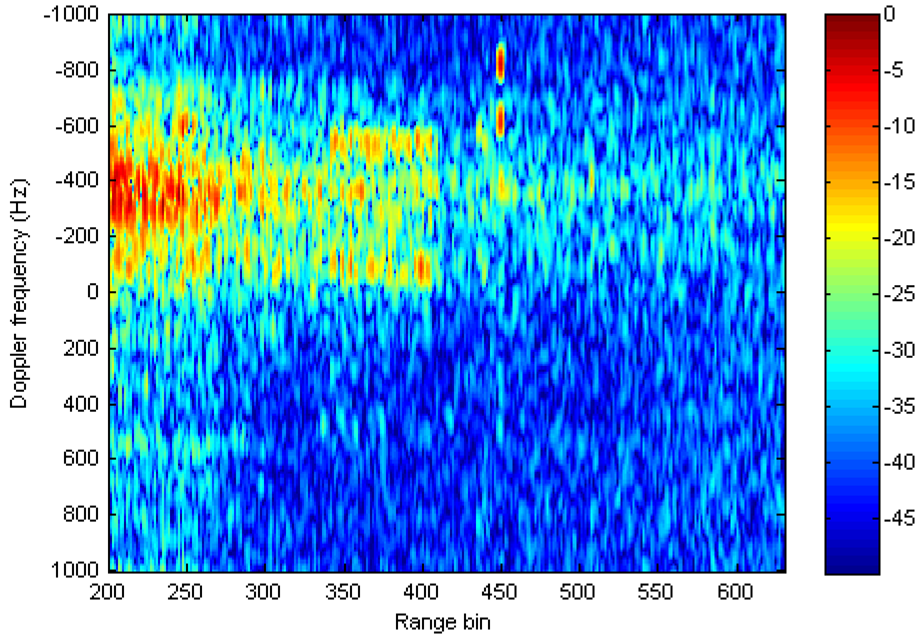

(b) PSTAP (RE050155, RE050152)

Figure 21: Range-Doppler maps of RE050152, processed by (a) STAP and (b) PSTAP. The moving target simulator (MTS) signals in range bin 450 are observed by both processors. PSTAP used the covariance matrix estimated from another dataset, RE050155.

7.2 Eigencanceller

Using the eigen-decomposition technique, the covariance matrix can be expressed as,

$$\mathbf{R}_u = \sum_{i=1}^{r_R} \lambda_i \mathbf{e}_i \mathbf{e}_i^H + \sum_{i=r_R+1}^{MN} \lambda_i \mathbf{e}_i \mathbf{e}_i^H = \mathbf{E}_i \mathbf{\Lambda}_i \mathbf{E}_i^H + \mathbf{E}_n \mathbf{\Lambda}_n \mathbf{E}_n^H \qquad (28)$$

where the eigenvectors have been sorted in such a way that the first r_R eigenvectors span the clutter subspace and the remains are for the thermal noise. Eigenvalues of clutter are assumed to be larger than that of thermal noise and $\mathbf{\Lambda}_n = \sigma^2 \mathbf{I}$ for white thermal noise.

It is well-known that the orthogonal projection can cancel interference if one chooses a projection matrix orthogonal to the interference (Klemm 2002, Chapter 1). Since eigenvectors of $\mathbf{E}_i$ and $\mathbf{E}_n$ are mutually orthogonal, if one chooses an orthogonal projection matrix,

$$\mathbf{P} = \mathbf{E}_n \mathbf{E}_n^H \qquad (29)$$

it will cancel the interference (clutter) perfectly while preserving the dimension of the vector space. Because $\mathbf{E}_i \mathbf{E}_i^H + \mathbf{E}_n \mathbf{E}_n^H = \mathbf{I}$, (*29*) can be equally expressed as,

$$\mathbf{P} = \mathbf{E}_n \mathbf{E}_n^H = \mathbf{I} - \mathbf{E}_i \mathbf{E}_i^H \qquad (30)$$

The use of orthogonal projection techniques based on eigenvector decomposition is referred to as eigencanceller (Klemm 2002, Chapter 1; Haimovich 1996). The weighting vector determined by the orthogonal projection processing (OPP) is,

$$\mathbf{w}_{opp} = \mathbf{P}\,\mathbf{s} \qquad (31)$$

It can be shown that the OPP processor is also an optimal processor and achieves the same coherent processing gains for all Doppler frequencies except at the Doppler frequency of mainlobe clutter (the cross point of the clutter subspace and detection subspace shown in the spatial-frequency and temporal-frequency plane in Figure 2) (Dong 2010).

It is important to point out that the weighting vector $\mathbf{w}_{opp}$ becomes a zero vector if the steering vector spans on the interference subspace, i.e., $\mathbf{s} \in \mathbf{E}_i$ ($\mathbf{s} = \sum_{i=1}^{r_R} s_i \mathbf{e}_i$, s_i is an arbitrary coefficient), one of the properties of orthogonal projection. In the detection subspace depicted in Figure 2, the point corresponding to zero spatial frequency and zero Doppler frequency also belongs to the interference subspace. Hence a target in the mainlobe direction with the same Doppler of the mainlobe clutter will become non-detectable regardless of its radar cross-section (RCS). This is fundamentally different from STAP. In STAP, the processor places a notch in the interference direction with an exact depth required to suppress the clutter. Therefore a target in the mainlobe direction with the same Doppler of mainlobe clutter is still detectable by STAP provided its RCS is larger than that of the clutter. On the other hand, the depth of the notch OPP places in the interference direction is infinite. Therefore, OPP detection does not allow the detection of targets having the same Doppler of the mainlobe clutter. Some other means have to be incorporated to include this detection. However, methods for detection of such targets are simple and straightforward, and do not need any sophisticated processing such as STAP.

This fundamental difference between STAP and OPP may be best explained by a SINR comparison shown in Figure 22. To suppress clutter, both processors place a notch at the Doppler of the mainlobe clutter (the target detection direction). The difference lies that the depth of the notch STAP placed is equal to the mainlobe CNR, so any target having higher RCS than the mainlobe clutter is still detectable. On the other hand, the depth of the OPP notch is infinite, and a target having the same Doppler as the mainlobe clutter and in the mainlobe direction is undetectable (Dong 2010).

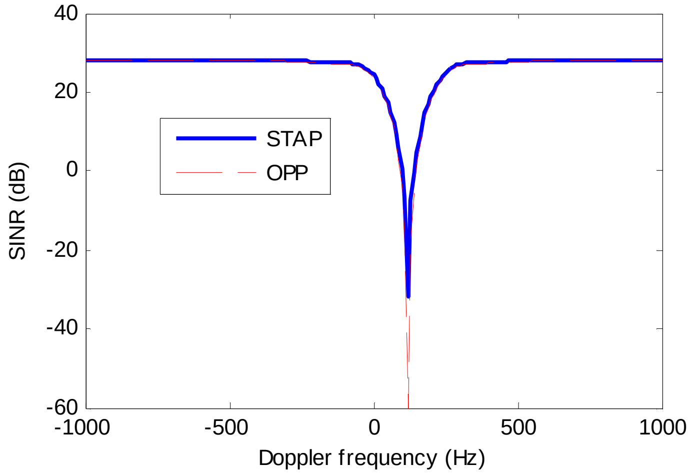

Figure 22: SINR comparison between STAP and OPP

Since the STAP is also meant to detect target having the same Doppler frequency as the mainlobe clutter (though there will be a significant SINR loss at the mainlobe clutter Doppler), it requires knowledge of both the structure (eigenvectors) and the strength (eigenvalues) of the covariance matrix, as,

$$\mathbf{w}_{opt} = \mathbf{R}_u^{-1}\mathbf{s} = \left(\sum_{i=1}^{r_R} \lambda_i^{-1} \mathbf{e}_i \mathbf{e}_i^H + \frac{1}{\sigma^2} \sum_{i=r_R+1}^{MN} \mathbf{e}_i \mathbf{e}_i^H \right) \mathbf{s} \qquad (32)$$

On the other hand, OPP does not include the detection of targets having the same Doppler frequency of the mainlobe clutter. Hence the weighting vector $\mathbf{w}_{opp}$ of (*31*) only requires the structure (eigenvectors) of the covariance matrix. Changes in eigenvalues of clutter do not have any influence on OPP! The eigenvalues are largely determined by the backscatter coefficients, or alternatively the single-element, single-pulse CNR for every clutter patch which is normally unknown a priori. Therefore, the use of OPP could provide an advantage in practice, as the unknown backscattering coefficients can be assumed to have arbitrary values without any sacrifice to the performance of the processor.

In general eigenvector decomposition is more computationally expensive than matrix inversion. Therefore OPP initially does not seem to have any computational advantage over STAP, if the corresponding weights need to be calculated from the same CPI data. Under the pseudo-STAP architecture, it is proposed to construct OPP weights using either clutter modelling or previous CPI data (Dong 2010).

Whether it is through mathematical modelling or estimation from secondary data, construction of OPP weights is simpler. If the weights are constructed through the mathematical modelling, the unknown clutter backscattering coefficients, the most difficult part of the clutter modelling can be assumed to have arbitrary values. If eigencanceller is constructed using previous CPI data, the requirement that the clutter environments of previous CPI and current CPI are better to be the same or similar can be relaxed. Different clutter environments may only alternate eigenvalues that, however, have no effects on forming the eigencanceller. Below we show a few results to demonstrate the performance of off-line eigencanceller.

Figure 23 shows detection test statistic for a RLSTAP dataset resulted from STAP and offline OPP. The offline OPP weights in this example were constructed using a clutter model, assuming nothing about the clutter environment is known except the radar and platform parameters. Note that all three targets are equally well detected by both detectors. Overall, the level of clutter residuals of OPP is statistically a few dB lower, since the clutter covariance matrix estimated by STAP using a limited number of non-homogeneous range samples would cause some SINR loss for STAP. A deep notch at the Doppler of the mainlobe clutter is also seen for OPP, one of features of OPP as discussed.

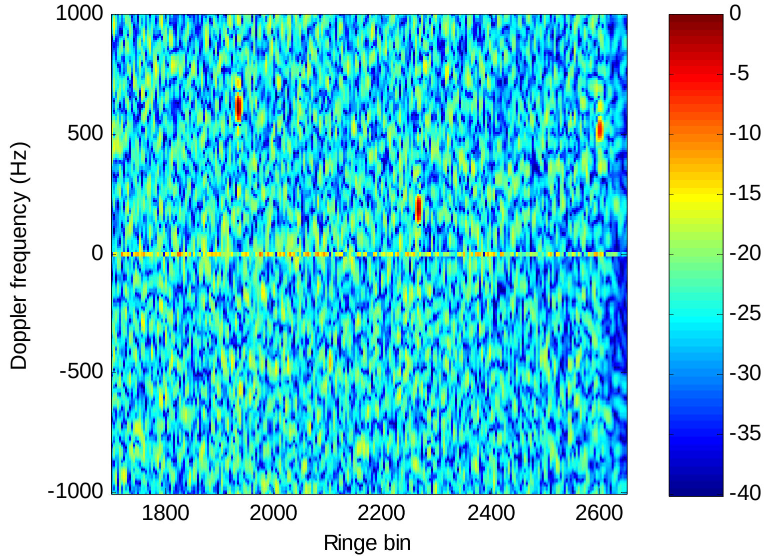

(a) STAP

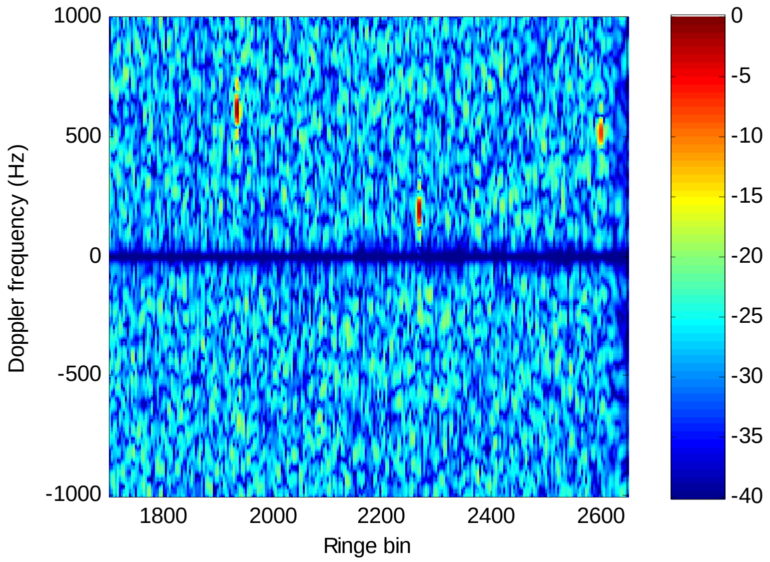

(b) OPP

Figure 23: Test statistics of (a) STAP and (b) OPP. The OPP weights were constructed using a clutter model, and no sample data was involved.

STAP test statistics for MCARM medium PRF RD050575 is shown in Figure 24, where three targets were detected. Of them, the target in range bin 299 was a genuine moving target while the other two targets in range bins 350 and 450, respectively, were injected artificial moving targets. Strong clutter residuals along the mainlobe clutter Doppler are seen possibly due to not sufficient samples in estimating the covariance matrix, and the heterogeneity of the real clutter environment. Note that the mainlobe clutter has non-zero Doppler frequencies, due to a crab angle.

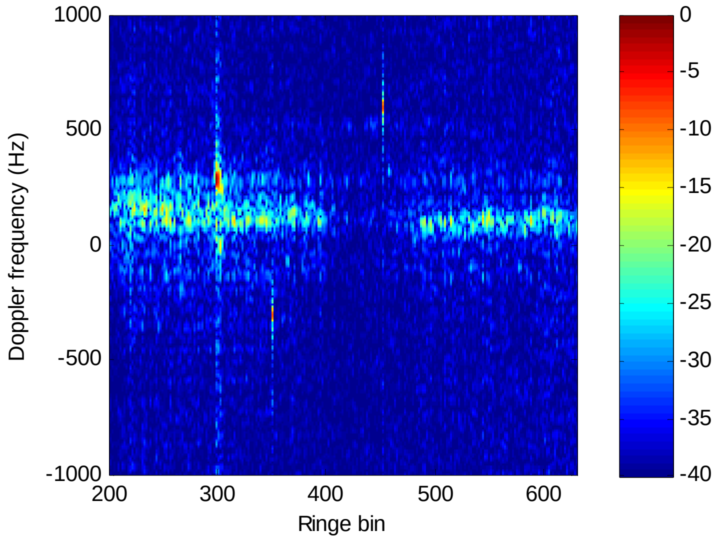

Figure 24: 'Real-time' STAP test statistics for MCARM RD050575. Three targets are all detected.

Test statistics of the 'real-time' OPP (i.e., using the same secondary data as STAP to construct the OPP weights) are shown in Figure 25(a). It can be seen that the OPP has greater capability to suppress clutter. This could be an advantage of 'real-time' OPP over STAP at the cost of higher computational demand. The results of offline OPP (i.e., using clutter modelling) are shown in Figure 25(b). It shows that the modelling OPP does not perform as well as 'real-time' OPP for genuine radar data. This is because, many effects, such as imperfection of radar calibration, near field interferences between radar and platform and so on were not counted in the modelling. Therefore, for a real radar system, using previous CPI data to construct offline OPP is preferred to avoid complexity of mathematical modelling. It is expected that if a previous dataset, which had the same radar and platform parameters as RD050575, the result of offline OPP would have been the same as Figure 25(a). Unfortunately, DSTO does not have such a dataset. However, DSTO do have other MCARM datasets which have the same radar parameters and similar platform parameters. These have been used to demonstrate the performance of offline OPP (Dong 2010).

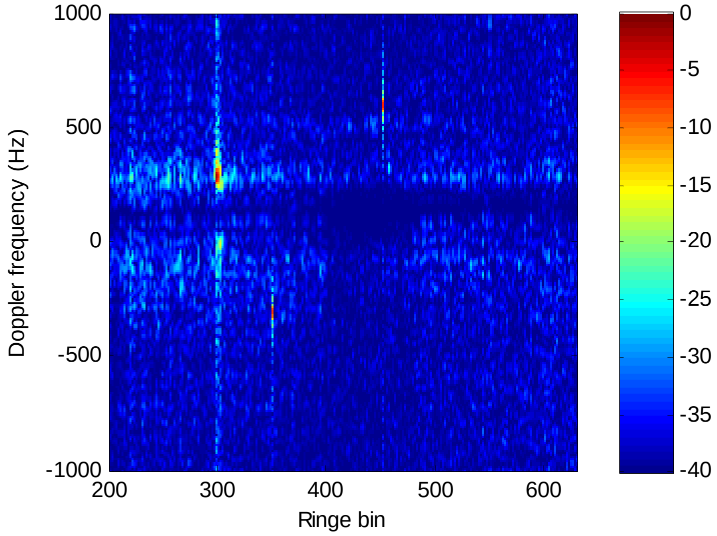

(a) 'real-time' OPP

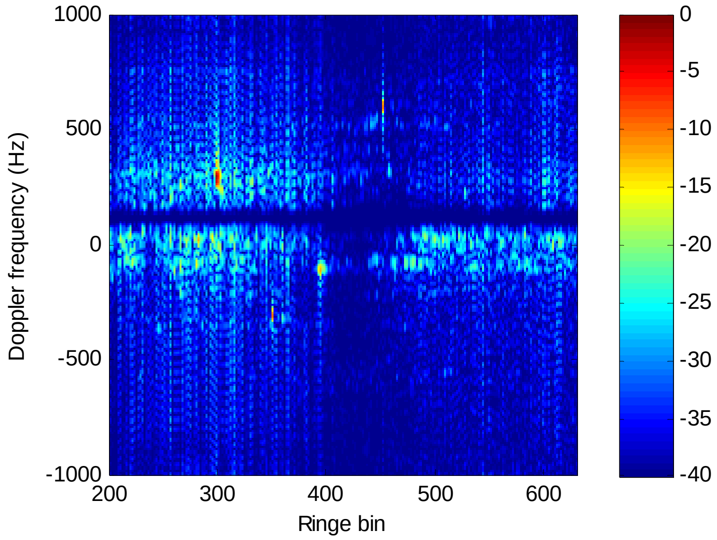

(b) 'offline' OPP

Figure 25: Test statistics of (a) 'real-time' OPP and (b) 'offline' OPP for MCARM RD050575

The STAP test statistic for RE050152 is shown in Figure 26(a), where the MTS signal in range bin 450 is shown. The offline OPP weights were constructed using RE050155 that has the same radar parameters and similar platform parameters. The corresponding detection results are shown in Figure 26(b). As shown, the offline OPP has a greater capability for clutter suppression.

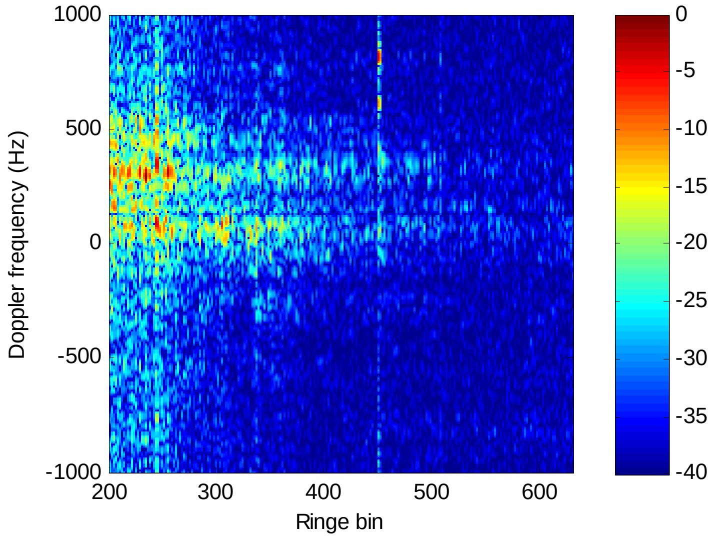

(a) 'real-time' STAP

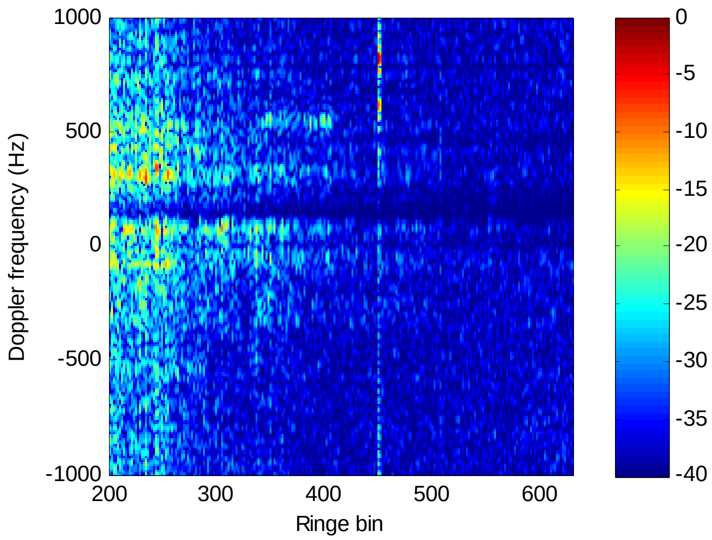

Figure 26: (a) STAP test statistic and (b) offline OPP test statistic of RE050152. The offline OPP weights were constructed using the same amount of range samples from RE050155.

The final example show in Figure 27 is the detection test statistic for MCARM low PRF RE050045. It is believed that there is no moving target in this dataset, and therefore, two artificial 0dB SNR moving targets were injected in range bins 700 and 900, respectively. The results of offline OPP constructed using the same amount of range samples from RE050046 and RE050047 are shown in Figure 28 (a) and (b), respectively.

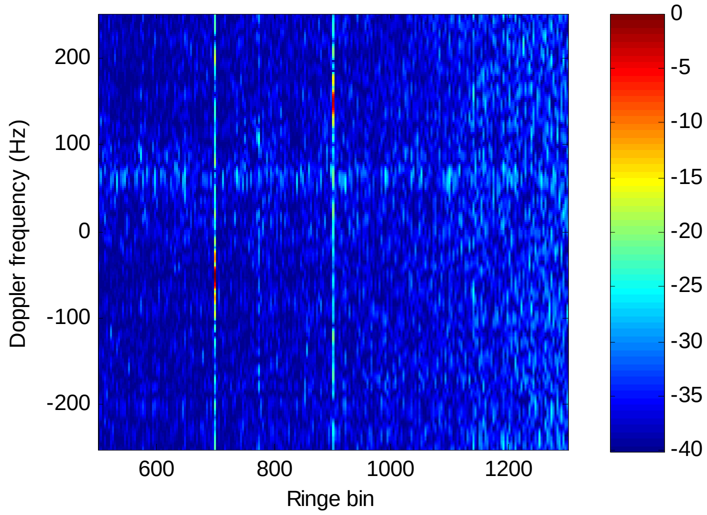

Figure 27: 'Real-time' STAP test statistic for RE050045

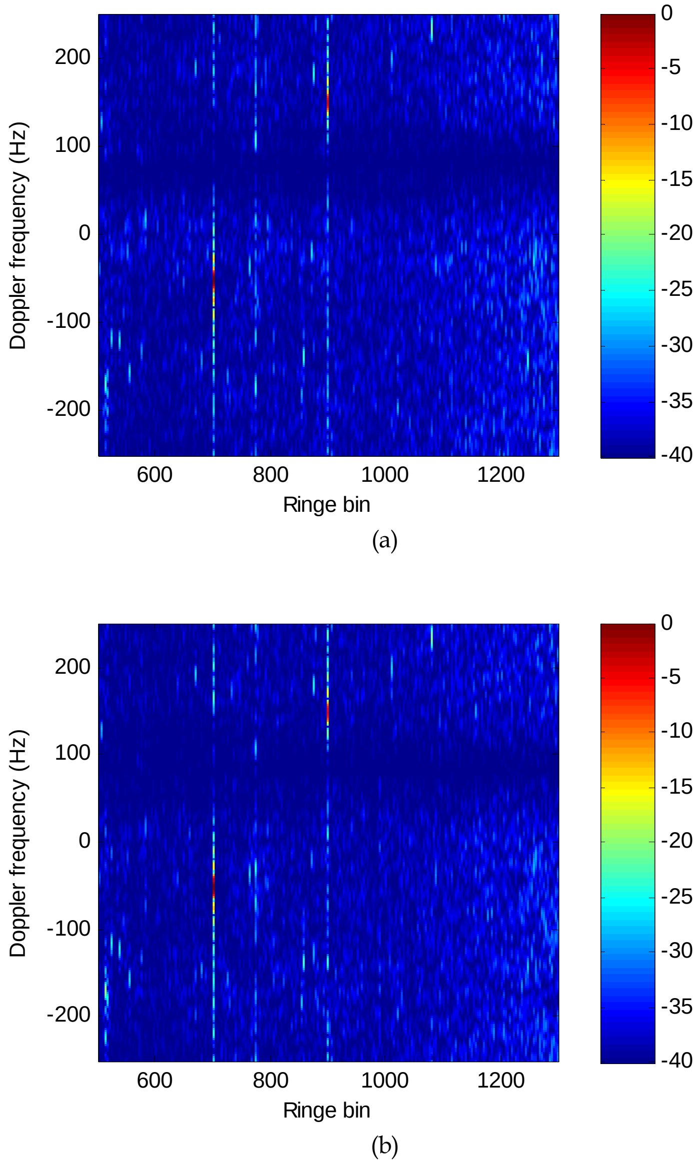

Figure 28: 'Offline' OPP test statistic for RE050045. The weights were constructed using the same amount of range samples from (a) RE050046 and (b) RE050047, respectively.

The above examples demonstrate that offline OPP constructed from previous CPI data perform approximately the same as or sightly better than STAP. Often STAP results higher residuals of mainlobe clutter due to insufficient suppression. On the other hand, because OPP orthogonally rejects mainlobe clutter, it has a much greater capability for clutter suppression and results in much lower clutter residuals.

7.3 Summary

Pseudo-STAP uses previous CPI data to estimate the covariance matrix and construct the optimal or near optimal weights accordingly. Using simulated datasets and genuine airborne radar datasets, it has been demonstrated that the performance of pseudo-PSTAP, (PSTAP) and offline OPP, are approximately the same as STAP, and no significant SINR loss occurs. To conduct a fair comparison, the size of training samples used by STAP, PSTAP and offline OPP was chosen to be the same. Since pseudo-STAP may have more training samples, it is possible that it can outperform STAP in theory.

Whether pseudo-STAP works or not depends on the condition match of the CPI data used for construction of the weights and the CPI data to be processed. The match here refers to radar and platform parameters. The match of the clutter environment is largely not required. This is because, (i) the inverse of the covariance matrix is approximately invariant for PSTAP and (ii) knowledge of the eigenvalues is not required for OPP.

The robustness of pseudo-STAP needs further investigation. It is found that among many radar and platform parameters, the crab angle plays a critical role in the success of PSTAP and OPP. Since the crab angle determines the centre frequency of the mainlobe clutter. If the measurement of the crab angle is not accurate, PSTAP and OPP could place the clutter notch in the wrong position, causing higher clutter residuals and significant false-alarms breakthrough. Further study is required whether potential subtle position changes between antenna panel and fuselage or wings of the platform (due to wind, fuel level change, etc) can significantly alter near field interferences which lead to significant changes in the covariance matrix and hence limit or degrade the performance of pseudo-STAP[6].

[6] Or even STAP if the variations are rapid relative to the CPI length.

8. 3D Data Processing

We have so far only focused on 2D space-time or azimuth-Doppler data processing. Airborne phased arrays typically are of a rectangular latticed structure. Data of antenna elements in elevation, if available, provides another dimension of processing, leading to so-called 3D data processing, i.e., elevation-azimuth-Doppler data processing. Adding elevation processing under some conditions can offer significant clutter suppression improvement, allowing further suppression of interference sources that have identical azimuth and Doppler. Obviously, when the number of elements in elevation reduces to one, the processing becomes the classical 2D space-time processing. Figure 29 depicts 1D and 2D array configurations of receiver.

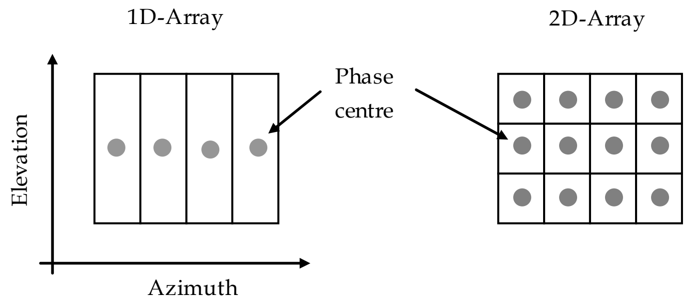

Figure 29: Two receive array configurations: 1D-array capable for 2D azimuth-Doppler processing and 2D-array for 3D elevation-azimuth-Doppler processing

Theoretically, the achievement of further clutter suppression by adding elevation processing is twofold. First for close range bins, airborne targets and the ground clutter may have different elevation angles as shown in Figure 30. Adaptive beamforming processing in elevation thus can separate target signals from undesired signals, providing clutter suppression in elevation domain.

Secondly, when radar is operated in medium and high PRF modes, the range is often ambiguous. If radar's look direction is not strictly boresight (due to either an existing crab angle or radar's beam being steered off the boresight), the Doppler of the ground clutter becomes range dependent. It means that the Doppler frequency of the unambiguous range clutter received by the mainlobe differs from the Doppler frequency of the ambiguous rang clutter received by sidelobes. For 2D STAP, the existence of ambiguous range clutter widens the Doppler spectrum of the mainlobe clutter. As a result, the STAP has to widen its clutter notch in the Doppler domain to null the clutter, which also induces an extra SINR loss for target detection. Since the ambiguous clutter enters the receiver via its sidelobes, differs from unambiguous range clutter which enters the receiver via its mainlobe, a proper adaptive processing in the elevation domain again can filter out the ambiguous range clutter to improve SINR in Doppler regions degraded by the ambiguous range clutter.

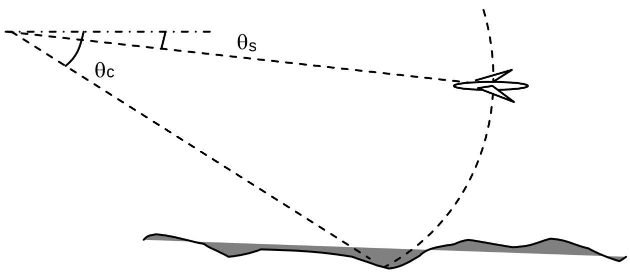

Figure 30: Elevation angles for an airborne target and the ground clutter may be significantly different for a close range bin

The steering vector for 3D STAP processing may be defined as,

$$\mathbf{s} = \mathbf{s}_e \otimes \mathbf{s}_t \otimes \mathbf{s}_s \tag{33}$$

where $\mathbf{s}_e$ represents the spatial steering vector in elevation, $\mathbf{s}_t$ and $\mathbf{s}_s$ denote the temporal steering vector in Doppler and the spatial steering vector in azimuth, respectively. The corresponding data snapshot is also stacked accordingly. Therefore, the previously discussed 2D STAP and its various variants can be readily extended to 3D without any difficulty.

Adding another dimension in STAP significantly enlarges the size of the covariance matrix, and hence its requirement for sample data support and computational budget also increases significantly accordingly.

Fertig and Krich (2005) show the benefits of 3D-STAP for small moving target detection using simulated airborne datasets. They demonstrate that the mainlobe clutter notch with respect to Doppler broadened by ambiguous range clutter in traditional 2D-STAP can be narrowed once 3D-STAP is employed. As a result, the degraded the minimum detectable velocity (MDV) of 2D-STAP is improved by 3D-STAP as shown in Figure 31. To examine the improvement of the detection performance, 24 0dB SNR moving targets with various Doppler were injected into a simulated X-band airborne radar dataset. As shown in Figure 32, while 2D-STAP managed to detect 11 out of the total 24, the 3D-STAP was able to detect 18 for the same threshold. It can be seen that the extra targets detected by 3D-STAP are those whose Doppler frequencies are close to that of the ambiguous range clutter.

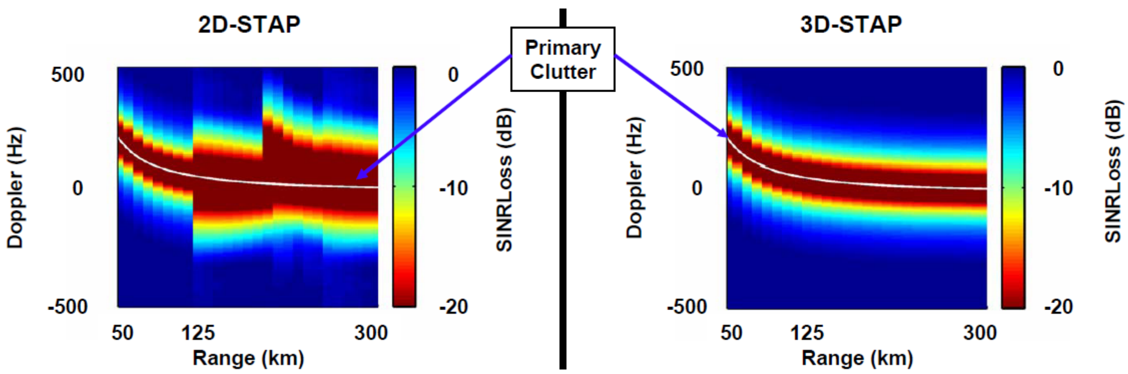

Figure 31: MDV degraded by ambiguous range clutter in 2D-STAP and its recovery in 3D-STAP (Fertig and Krich, 2005)

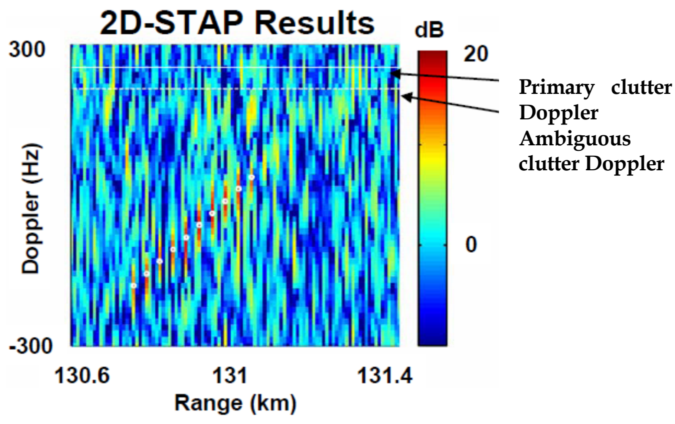

(a) 2D-STAP

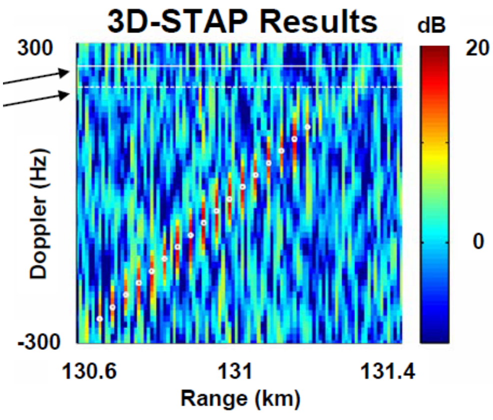

(b) 3D-STAP

Figure 32: Detection result comparison using 2D- and 3D-STAP. More targets are detected using 3D-STAP. The detected targets are marked by white dots (Fertig and Krich, 2005).

Similar to the mainlobe clutter, the sidelobe clutter is also correlated to the Doppler. Therefore, all three dimensions are mutually correlated. That is, the clutter covariance matrix of 3D STAP is strictly inseparable. Any separate processing or dimension-reduced processing inherently leads to suboptimal processing associated with a SINR loss.

A hybrid 3D-STAP architecture is proposed by Hale et al (2002). In order to reduce the size of dimension, the 3D problem is simplified to three cascaded processing stages as shown in Figure 33. It can be seen that it is an extension of traditional 2D factored time-space technique (FTS), and the beamforming in elevation as the first-stage is added. The 2D FTS technique is also popularly referred to as adaptive element-space post-Doppler processing. As stated, since the clutter covariance matrix is inseparable, this sub-optimal processing simplification is associated with a SINR loss, predominately in the Doppler region close to the Doppler of the mainlobe clutter. Nevertheless, through tests on simulated datasets, the authors demonstrated that 17-20dB SINR improvement can be achieved based on the test using their simulated datasets where ambiguous range clutter exists. The authors claim that the SINR loss inherently incurred in the 2D FTS method can be effectively mitigated or reduced by adding the elevation processing without increasing secondary data support (since the dimension of the adaptive part remains the same). Improved performance over a 2D full STAP was also demonstrated by adding the elevation processing for the range unambiguous clutter case.

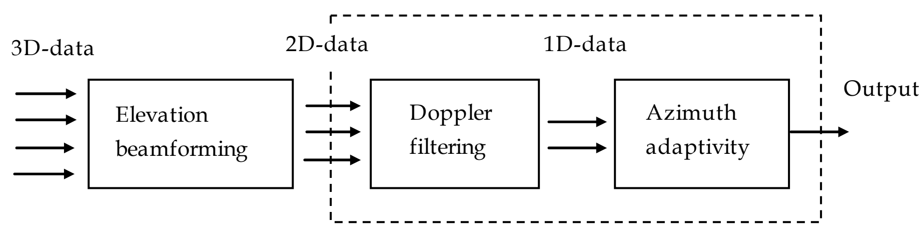

Figure 33: Hybrid 3D architecture incorporating elevation beamforming proposed by Hale et al (2002)

9. Effects of Imperfections of Radar-Platform System

While adaptive processing may be able to mitigate effects of some imperfections of radar-platform system, so far the effects on the radar performance have not yet been explicitly discussed.

Phased-array radar is a complex system. Its amplitude and phase calibration is a challenge process for the radar industry because of mutual coupling among array elements. When the array is mounted onto a platform, the radar-platform system becomes even much more complex and difficult to calibrate, because there are unavoidable near-field interferences between the array and the platform. In consequence, channel imperfect calibration, channel mutual leakage, near field interference are all contributing factors that not only alter the clutter covariance matrix but also degrade radar performance in some cases. Some effects of imperfections have been discussed (Guerci 2003, Chapter 4; Dong 2008).

The overall imperfections may be represented by a calibration error for each channel, and may be divided into three types (Dong 2008).

Type 0 error – the calibration error is unknown but remains constant over an extended period (many CPIs). This kind of error may be measured /compensated by data processing or addressed by pseudo-adaptive processing and history based training.

Type I error – the calibration error is random, unknown but remains constant for all pulses in a CPI. This error in general does not incur a significant SINR loss in adaptive processing. On the transmitting side, the calibration error distorts the beam pattern, notably a lower mainlobe and higher sidelobes. The lower mainlobe usually results in a lower return of the target signal and consequently a loss of SINR. However, the deterioration of the mainlobe in general should be within a few dB for a realistic radar system. On the receiving side, the higher sidelobes resulting in higher clutter returns. However, STAP is able to suppress clutter. Therefore, for adaptive processing, this type of error does not cause any significant SINR loss.

Type II error – the calibration error is random, unknown and varying from pulse to pulse for a CPI. The effect of this type of error is usually twofold. First, it increases the number of eigenvalues of the clutter covariance matrix, and hence requires more sample data to support adaptive processing. Secondly, it increases the system's noise floor. For a perfectly calibrated system, the noise floor (uncorrelated and uniformly distributed in the space-time domain) is only the thermal noise of the system. Type II error could equivalently produce a white-noise-like component, acting like the thermal noise, and hence increases the system's noise floor. Since white noise is not suppressible, Type II error calibration may result in a significant SINR loss.

Imperfections of the radar-platform system also limit many processing algorithms and strategies. STAP is all about the suppression of sidelobe clutter. If calibration of the radar-platform system can be achieved at a high level, a proper set of tapering coefficients (window functions) for the transmitting array can in the first place lower the sidelobes of the transmitting beam pattern, which in turn produces low sidelobe clutter, and mitigate the SINR loss caused by sidelobe clutter. In addition, for a perfectly calibrated system one may also design special sets of tapering coefficients to form a deep notch at a sidelobe azimuth of the receive sum beam to filter out the clutter component having the associated Doppler. This is shown in Figure 34. The resulted signal of the sum channel, if having that Doppler component, can only be generated by target from the mainlobe direction but not the clutter. In this way, there is no need to perform Space-time processing as the clutter has been suppressed. Repeating the processing by shifting the clutter notch over the whole sidelobe clutter azimuth will detect all targets in the sidelobe clutter Doppler region with the only competition of thermal noise. However, this requires a precise if not perfect calibration. Any small calibration error will usually not result in the desired deep notch.

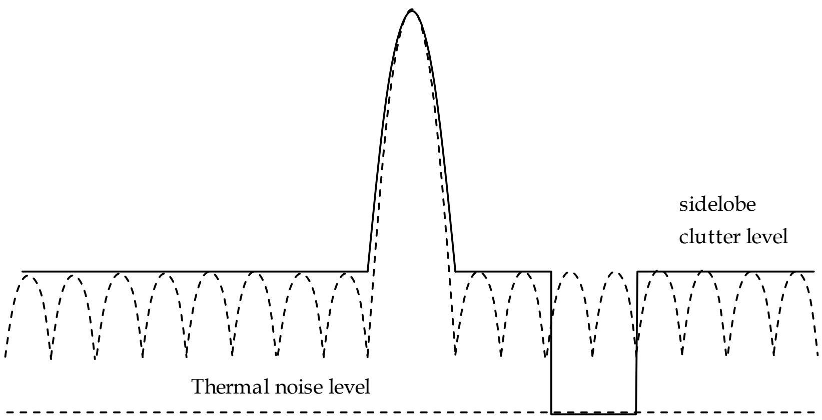

Figure 34: A special receive sidelobe level design (solid-line) in comparison with the normal pattern design (dashed-line). The notch excludes the clutter component (associated with a specific Doppler frequency band) from the received sum beam signals and hence achieves clutter suppression.

10. Overview

STAP obtains an optimal coherent processing gain of $10\log_{10}(MN)$ dB with respect to the thermal noise floor for target signals in all Doppler bins except the Doppler bin(s) of the mainlobe clutter (assuming the mainlobe direction is the detection direction). It means that the processor should be capable of suppressing clutter in Doppler bins of sidelobe clutter by the amount of CNR for those Doppler bins. For radar operated in the high PRF mode, there are also Doppler bins that are clutter-free, and the processing of these bins does not require any clutter suppression, and hence is relatively straightforward and simple.

The key processing principle for clutter suppression is space-time processing. Under the detection scenario, a target is supposed to be in the mainlobe direction, different from a sidelobe direction from which clutter having the same Doppler as the target is being received. To achieve clutter suppression in such a scenario, the sufficient and necessary conditions are:

(i) received signals to contain spatial information; and

(ii) a processor to be able to separate spatially different signals.

Satisfaction of the first condition is often achieved by using a linear phased array in the azimuth direction. The realisation of the second condition needs involvement of space-time processing, since unfortunately the clutter covariance matrix is spatial-temporal inseparable.

Classical 'full STAP' using the diagonally-loaded covariance matrix inversion method provides optimal detection for Gaussian clutter but faces a few critical issues. Data and computational expenses are major concerns. Other potential risks include contamination of training data by targets and the training samples not being independent and identically distributed with respect to the cell under test.

Mainly to overcome the computational and data expense requirements, quite a significant number of simplified sub-optimal STAP variants have been developed and proposed in the literature over the last 30 years.

The majority of these sub-optimal STAP variants fall in the category of dimension-reduced STAP. While details of these algorithms may vary from one to the other, they share the same or similar concepts and achieve similar results. The most data resource efficient and computation efficient, among other sub-optimal STAP algorithms, and the best representative of them, as far as the author's awareness, might be the so-called joint-domain localised STAP, which has be reviewed in this paper, and details of the others are skipped.

Parametric adaptive matched filter and adaptive displaced phase centre antenna utilise the linear autoregressive technique to whiten and decorrelate space-time correlated clutter to simplify the processing. These algorithms are both data resource efficient and computation efficient.

Representatives of rank-reduced STAP, such as the principle component method and multi-stage Wiener filter aim at achieving data resource efficient which is often critical especially in a heterogeneous clutter environment and for data resource limited cases. However, the realisation of these algorithms demands even more computation than classical STAP at this stage. How to simplify these algorithms to make them computation efficient needs further research.

The idea of pseudo-STAP algorithms is to select training samples from historical measurements to ease the problem of lack of sufficient training data and to shift massive calculation of optimal weights to offline. The key to success of these algorithms is the match of the radar and platform parameters between the training data and the data to be processed. Parameter discrepancies (explicitly or implicitly) between training data and data to be processed may incur significant degradation of the performance. Differences in clutter environments between the training data and the data to be processed have ignorable effects on the detection performance.

Knowledge-aided STAP is an architecture rather than an algorithm. Its application with STAP algorithms can result in improvement of detection performance. While its applications are versatile, one of its applications discussed is to assist in selection of training samples particularly in the heterogeneous clutter environment to exclude potentially contaminated or non iid samples using prior knowledge. There is no free lunch, adding the knowledge information system into the processing certainly increases the complexity of the detection problem and requires more computation power to resolve.

There might be no single algorithm that consistently performs best for all scenarios. Detection strategies might be designed and planned in such a way in which various detectors are to be used in different scenarios depends on the computation power and the data resource available to the system. For instance, during a manoeuvre transition period, it might not be desirable to use range samples for estimating the weights. Conducting a simple Fourier transform with an appropriate window function to lower sidelobe clutter for detection might be a fast and feasible solution. Bearing in mind though, this kind of detection is associated with a SINR loss of CNR varying with Doppler bin to Doppler bin. During a stable and level flying period, if clutter environment is relatively homogeneous and there are sufficient training data, partial STAP or full STAP may be employed depending on the computation power available to the system. If the system is in a routine cruise mission, repeats its surveillance routes, and operators are confident about radar and platform parameters, pseudo-STAP may be used.

Finally features of the above discussed STAP algorithms are briefly summarised in Table 1.

Table 1: Features of STAP algorithms

Category	Representative algorithm	Requirement of Training data	Requirement of Computation	SINR loss	Risk	Comments
Full STAP	Diagonall-loaded covariance matrix inversion	Very high	Very high	Low	In heterogeneous clutter area, insufficient training data to support could cause high SINR loss	Knowledge-aided system helps to select proper training data to improve performance. This is also applicable to all other algorithms.
Dimension-reduced STAP	Joint-domain localised STAP	Low	Low	Medium	High SINR loss can occur in Doppler bins close to the mainlobe clutter	It is a both data resource and computationally efficient algorithm.
	Parametric adaptive matched filter	Medium	Medium	Low	High SINR loss can occur in Doppler bins close to the mainlobe clutter	The effective number of pulses will be reduced leading to a dimension loss. If the number of pulses in a CPI is low, one can use the modified PAMF to avoid the dimension loss.
	Adaptive displaced phase centre antenna	Medium	Medium	Low	High SINR loss can occur in Doppler bins close to the mainlobe clutter	It is even more data resource and computation efficient algorithm than PAMF. The disadvantage is that the number of effective antenna elements is reduced by one and the number of effective pulses is also reduced by 1.
	ΣΔ-STAP	Low	Low	High	Suppression of targets close to clutter	It does not require received signals to be recorded at the antenna element level. The SINR loss is equal to CNR of the Doppler bin.
Rank-reduced STAP	Principle component method and multi-Wiener filter	Medium	Very high	Low	Insufficient training data support results in high SINR loss	The computation cost is even higher than the full STAP.
Pseudo-STAP	Pre-built STAP and offline eigencanceller	None (see comment 2)	very low (see comment 3)	Low	Discrepancies between the measured parameters and the actual parameters could lead to significant SINR loss.	1. High accuracy of radar and platform parameters is required, which may not be required by other adaptive algorithms. 2. The requirement of training data is very high, but fulfilled by historical measurements. 3. The computational cost is also very high, but shifted to offline and transformed to a data storage cost for each flight conditions. 4. The success of these algorithms depends on the match of the radar and platform parameters (explicitly and implicitly) for the training data and the data to be processed.

11. Acknowledgement

The author thanks Dr A. P. Shaw for his various comments.

12. References

Blum, R. S., Melvin, W. L., and Wicks, M. C. (1996), "An analysis of adaptive DPCA", *Proceedings 1996 IEEE National Radar Conference*: 303-308.

Brennan, L. E., and Reed, I. S. (1973), "Theory of adaptive radar", *IEEE Trans. on Aerospace and Electronic Systems*, **AES-9**, 237-252.

Brennan, L. E., and Staudaher, F. M. (1992), "Subclutter visibility demonstration", Technical Report, RL-TR-92-21, Adaptive Sensors Incorporated.

Capraro, C. T., Capraro, G. T., Bradaric, I., Weiner, D. D., Wicks, M., and Baldygo, W. J. (2006), "Implementing digital terrain data in knowledge-aided space-time adaptive processing", *IEEE Trans. on Aerospace and Electronic Systems*, **42**(3), 1080-1099.

Capraro, G. T., and Wicks, M. (2004), "An Airborne Intelligent Radar System", *International Conference on Radar Systems*, Toulouse.

Capraro, G. T., and Wicks, M. (2010), "Metacognition in Radar", *International Conference on Electromagnetics in Advanced Applications*, Sydney: 693-696.

De Greve, S., Ries, P., Lapierre, F. D., and Verly, J. G. (2007), "Framework and taxonomy for radar space-time adaptive processing (STAP) methods", *IEEE Trans. on Aerospace and Electronic Systems*, **43**(3), 1084-1099.

Dong, Y. (2005a), "Approximate invariance of the inverse of the covariance matrix and the resultant pre-built STAP processor", Research Report, DSTO-RR-0291, Defence Science and Technology Organisation, Australia.

Dong, Y. (2005b), "Evaluation of pre-built space-time non-adaptive processing (PSTAP)", Research Report, DSTO-RR-0295, Defence Science and Technology Organisation, Australia.

Dong, Y. (2006), "Parametric adaptive matched filter and its modified version", Research Report, DSTO-RR-0313, Defence Science and Technology Organisation, Australia.

Dong, Y. (2007), "Phased array radar data processing using adaptive displaced phase centre antenna principle", Research Report, DSTO-RR-0334, Defence Science and Technology Organisation.

Dong, Y. (2008), "Effects of antenna inperfections on STAP performance", DSTO Discussion Paper, DSTO-DP-1121, Defence Science and Technology Organisation, Australia.

Dong, Y. (2010), "Eigencanceller in space-time adaptive processing for airborne radar", Technical Report, DSTO-TR-xxxx, Defence Science and Technology Organisation, Australia.

Fertig, L. B., and Krich, S. I. (2005), "Benifits of 3D-STAP for X-band GMIT airborne radars", *Adaptive Sensor Array Processing (ASAP) Workshop*, MIT, MA.

Goldstein, J. S., Reed, I. S., and Scharf, L. L. (1998), "A multistage representation of the Wiener filter based on orthogonal projections", *Information Theory, IEEE Transactions on*, **44**(7), 2943-2959.

Guerci, J. R. (2002), "Knowledge-aided sensor signal prrocessing and expert reasoning", *Knowledge-Aided Sensor Signal Processing and Expert Reasoning (KASSPER) Workshop*, Washington, DC.

Guerci, J. R. (2003), *Space-Time Adaptive Processing for Radar*, Boston, Artech House.

Guerci, J. R. (2004), "Knowledge-aided sensor signal processing and expert reasoning (KASSPER)", *KASSPER Work Shop*.

Guerci, J. R., Goldstein, J. S., and Reed, I. S. (2000), "Optimal and adaptive reduced-rank STAP", *IEEE Trans. on Aerospace and Electronic Systems*, **36**(2), 647-663.

Haimovich, A. (1996), "The eigencanceller: adaptive radar by eigenanalysis methods", *IEEE Trans. on Aerospace and Electronic Systems*, **32**(2), 532-542.

Hale, T. B., Temple, M. A., Wicks, M. C., Raquet, J. F., and Oxley, M. E. (2002), "Performance characterisation of hybrid STAP architecture incorporating elevation interferometry", *IEE Proc.~Radar, Sonar Navig.*, **149**(2), 77-82.

Haykin, S. (2006), "Cognitive radar", *IEEE Signal Processing Magazine*, 30-40.

Haykin, S. (2010), "Cognitive dynamic systems", *Short-Course Notes*, Adelaide, Australia.

Himed, B. (2008), "STAP techniques and applications (Tutorial)", *IEEE International Radar Conference*, Adelaide, Australia.

Klemm, R. K. (2002), *Principles of Space-Time Adaptive Processing*, 2nd, London, IEE.

Klemm, R. K., editor, (2004), *Applications of Space-Time Adaptive Processing*, London, IEE.

Li, J., and Stoica, P., editors (2006), *Robust Adaptive beamforming*, New Jercey, John Wiley & Sons.

Li, X. M., Feng, D. Z., Liu, H. W., and Bao, Z. (2008), "Spatial-temporal separable filter for adaptive clutter suppression in airborne radar", *Electronics Letters*, **44**(5).

Melvin, W., Wicks, M., Antonik, P., Salama, Y., Li, P., and Schuman, H. (1998), "Knowledge-based space-time adaptive processing for AEW radar", *IEEE AES Systems Magazine*, **13**(4), 37-42.

Melvin, W. L. (2004), "A STAP overview", *IEEE A&E Systems Magazine*, **19**(1), 19-35.

Page, D., Scarborough, S., Owirka, G., and Crooks, S. (2004), "Improving knowledge-aided STAP performance using past CPI data", *Preceedings of the 2004 IEEE Radar Conference, 26-29 April, Philadelphia***:** 295-300.

Reed, I. S., Mallett, J. D., and Brennan, L. E. (1974), "Rapid convergence rate in adaptive array", *IEEE Trans. on Aerospace and Electronic Systems*, **10**(6), 853-863.

Roman, J. R., Rangaswamy, M., Davis, D. W., Zhang, Q., Himed, B., and Michels, J. H. (2000), "Parametric adaptive matched filter for airborne radar applications", *IEEE Trans. on Aerospace and Electronic Systems*, **36**(2), 677-692.

Wang, H., and Cai, L. (1994), "On adaptive spatial-temporal processing for airborne surveillance radar systems", *IEEE Trans. on Aerospace and Electronic Systems*, **30**(3), 660-670.

Wang, H., Schneible, R. A., Brown, R. D., and Zhang, Y. (2004). "Chapter 4 ΣΔ–STAP: an effecient, affordable approach for clutter suppression", *Applications of Space-Time Adaptive Processing*, R. Klemm, London, IEE**:** 123-147.

Ward, J. (1994), "Space-time adaptive processing for airborne radar", Technical Report, 1015, Lincoln Laboratory, MIT.

Ward, J., and Kogon, S. M. (2004), "Space-time adaptive processing (STAP) for AMTI and GMTI radar", *Proceedings of 2004 IEEE Radar Conference*, Philadelphia, Pennsylvania.

Zywicki, D. J., Melvin, W. L., Showman, G. A., and Guerci, J. R. (2003), "STAP performance in site-specific clutter environment", *IEEE Aerospace Conference*, Big Sky, MT**:** 2005-2020.

DEFENCE SCIENCE AND TECHNOLOGY ORGANISATION DOCUMENT CONTROL DATA	1. PRIVACY MARKING/CAVEAT (OF DOCUMENT)

2. TITLE	3. SECURITY CLASSIFICATION (FOR UNCLASSIFIED REPORTS THAT ARE LIMITED RELEASE USE (L) NEXT TO DOCUMENT CLASSIFICATION)
Overview of STAP Algorithms	Document (U) Title (U) Abstract (U)
4. AUTHOR(S)	5. CORPORATE AUTHOR
Yunhan Dong	DSTO Defence Science and Technology Organisation PO Box 1500 Edinburgh South Australia 5111 Australia

6a. DSTO NUMBER	6b. AR NUMBER	6c. TYPE OF REPORT	7. DOCUMENT DATE
DSTO-TN-0992	AR-014-950	Technical Note	March 2011

8. FILE NUMBER	9. TASK NUMBER	10. TASK SPONSOR	11. NO. OF PAGES	12. NO. OF REFERENCES
2011/1034221	07/044	PM C&W	50	38

DSTO Publications Repository	14. RELEASE AUTHORITY
http://dspace.dsto.defence.gov.au/dspace/DSTO-TN-0992	Chief, Electronic Warfare and Radar Division

15. SECONDARY RELEASE STATEMENT OF THIS DOCUMENT

Approved for public release

OVERSEAS ENQUIRIES OUTSIDE STATED LIMITATIONS SHOULD BE REFERRED THROUGH DOCUMENT EXCHANGE, PO BOX 1500, EDINBURGH, SA 5111

16. DELIBERATE ANNOUNCEMENT

No Limitations

17. CITATION IN OTHER DOCUMENTS Yes

18. DSTO RESEARCH LIBRARY THESAURUS

space-time adaptive processing, airborne radar, phased array data processing, adaptive displaced phase centre antenna, parametric adaptive matched filter

19. ABSTRACT

This technical note reviews space-time adaptive processing (STAP) algorithms including various dimension-reduced, rank-reduced partial or sub-optimal variants as well as pseudo-STAP algorithms. Briefly examined are also knowledge-aided (KA) STAP and elevation-azimuth-time 3D STAP that further improve STAP performance, especially under the heterogeneous clutter environment and range ambiguous conditions. Imperfections of radar-platform system deteriorating performance and limiting detection algorithms are discussed. Requirements on data resource and computation by each algorithm are assessed and compared.